



Available online at www.sciencedirect.com

SCIENCE @ DIRECT®

Journal of Clinical Neuroscience 13 (2006) 661–665

Journal of
Clinical
Neuroscience

www.elsevier.com/locate/jocn

Laboratory study

14-3-3 protein levels and isoform patterns in the cerebrospinal fluid of Creutzfeldt-Jakob disease patients in the progressive and terminal stages

Yusei Shiga ^{a,*}, Hideki Wakabayashi ^b, Koichi Miyazawa ^a, Hiroshi Kido ^b,
Yasuto Itoyama ^a

^a *Department of Neurology, Tohoku University School of Medicine, 1-1 Seiryomachi, Aoba-ku, 980-8574 Sendai, Japan*

^b *Division of Enzyme Chemistry, Institute for Enzyme Research, University of Tokushima, Tokushima, Japan*

Received 17 May 2005; accepted 23 September 2005

Laboratory study

14-3-3 protein levels and isoform patterns in the cerebrospinal fluid of Creutzfeldt-Jakob disease patients in the progressive and terminal stages

Yusei Shiga ^{a,*}, Hideki Wakabayashi ^b, Koichi Miyazawa ^a, Hiroshi Kido ^b,
Yasuto Itoyama ^a

^a Department of Neurology, Tohoku University School of Medicine, 1-1 Seiryomachi, Aoba-ku, 980-8574 Sendai, Japan

^b Division of Enzyme Chemistry, Institute for Enzyme Research, University of Tokushima, Tokushima, Japan

Received 17 May 2005; accepted 23 September 2005

Abstract

To elucidate the diagnostic value and to establish the 14-3-3 isoform patterns in the cerebrospinal fluid (CSF) of Creutzfeldt-Jakob disease (CJD) patients, we analysed the 14-3-3 isoform patterns in the CSF of 11 CJD patients using the Western immunoassay technique. 14-3-3 protein was detected in the CSF of seven CJD patients in the progressive stage, but not in four patients in the terminal stages whose brains were severely atrophied. The amount of 14-3-3 protein measured semi-quantitatively in the CSF was correlated with that of neuron-specific enolase measured using an enzyme-linked immunosorbent assay in the same CSF. CJD patients showed five dominant 14-3-3 isoforms, γ , ϵ , ζ , η and β , but 14-3-3 τ , which mainly originates from T lymphocytes, was not detected. 14-3-3 protein is released into the CSF as a consequence of the extensive and rapid destruction of the brain, and the presence of the five isoforms enhances the diagnostic value of 14-3-3 protein in the progressive stage.

© 2006 Elsevier Ltd. All rights reserved.

Keywords: Creutzfeldt-Jakob disease; 14-3-3 protein; Isoform pattern; Neuron-specific enolase

1. Introduction

The detection of 14-3-3 protein in cerebrospinal fluid (CSF) is an important premortem immunoassay marker to support the diagnosis of Creutzfeldt-Jakob disease (CJD)¹ and is included in the World Health Organization (WHO) diagnostic criteria.² However, positive detection has been reported in various neurological disorders other than CJD,³ and such misleading results could lead to an erroneous diagnosis.⁴

14-3-3 protein has seven isoforms,⁵ and six isoforms have been detected in the mammalian brain.⁶ The 14-3-3 isoform patterns in the CSF of CJD patients have been reported,^{7,8} but the results are controversial, probably because of the inadequate isoform-specificities of the antibodies used in the experiments. To elucidate the diag-

nostic value of and to establish the 14-3-3 isoform pattern in the CSF of CJD patients, we evaluated the isoform patterns in the CSF of CJD patients in the progressive and terminal stages by using highly isoform-specific antibodies against 14-3-3 protein.⁹

2. Methods

We collected CSF from 11 CJD patients, including two familial cases of CJD with no family history of CJD nor dementia, and one patient who had received cadaveric dura mater during surgical resection of a right acoustic neuroma. The patients were aged between 55 and 79 years, with a mean age of 70.4 years. Seven were diagnosed with probable CJD, and four were definite cases based on the WHO diagnostic criteria.² In the seven patients with probable CJD (patients 1 to 7), lumbar CSF was collected in the progressive stage 1–6 months after onset, when the patients were admitted to our hospital, and was stored at $-80\text{ }^{\circ}\text{C}$

* Corresponding author. Tel.: +81 22 717 7189; fax: +81 22 717 7192.
E-mail address: yshiga@em.neurol.med.tohoku.ac.jp (Y. Shiga).

until analysis. Brain magnetic resonance imaging (MRI) studies of these seven patients were performed at the same time as the CSF collection and the results showed no brain atrophy in two, slight atrophy in three, and moderate atrophy in two patients. The CSF of the remaining four patients with definite CJD (patients 8 to 11; Table 1) was collected fresh in the terminal stages 1.5–4 years after onset and was stored at -80°C until analysis. The brain MRI scans of these four patients showed very severe brain atrophy, very thin cortices and white matter, and enormously dilated ventricles. The profiles of the patients enrolled in this study, including the clinical, laboratory, and radiological findings, are listed in Table 1.

To detect 14-3-3 protein in CSF, we initially analysed the CSF using the polyclonal rabbit antibodies SC-629 (Santa Cruz Biotechnology, Santa Cruz, CA, USA), which react to the common epitopes of all 14-3-3 isoforms (pan 14-3-3). To verify the isoform specificities of the 14-3-3 antibodies, we evaluated the cross-reactivities of the antibodies we raised against each 14-3-3 isoform⁹ and the commercially available antibodies by dot hybridisation as follows: six different recombinant isoforms (β , τ , η , ζ , ϵ , and γ ; 10 ng) were dotted onto a nitrocellulose membrane and incubated with the antibodies against 14-3-3 isoforms (β , τ , η , ϵ , and γ). The commercially available antibodies SC-628 for 14-3-3 β , SC-732 for 14-3-3 τ , SC-1019 for 14-3-3 ζ , SC-1020 for 14-3-3 ϵ , and SC-731 for 14-3-3 γ (Santa Cruz Biotechnology, Santa Cruz, CA, USA) were also evaluated.

Twenty μL of each CSF specimen was subjected to 10–20% gradient sodium dodecyl sulfate–polyacrylamide gel electrophoresis (SDS-PAGE), and then transferred onto an Immobilon P membrane (Millipore, Fremont, CA, USA) at 90 mA for 120 min. The membranes were subsequently treated with 3% skim milk (Yukijirushi, Sapporo, Japan) for 1 h at room temperature, and then reacted with SC-629 pan 14-3-3 antibodies and the isoform-specific antibodies (2 $\mu\text{g}/\text{mL}$ for SC-629, 14-3-3 γ , ϵ , η , β , and τ , and 0.2

$\mu\text{g}/\text{mL}$ for SC-1019) at 4°C overnight. The membranes were incubated with 1:5000 dilutions of horseradish peroxidase (HRP)-conjugated anti-rabbit immunoglobulin G (IgG; Zymed, South San Francisco, CA, USA) or 1:4000 dilutions of HRP-conjugated anti-mouse IgG (Dako, Carpinteria, CA, USA) for 1 h at room temperature. The immunoreactive bands were visualised on Fuji RX-U films (Fujifilm, Tokyo, Japan) using enhanced chemiluminescence (ECL) detection reagents (Amersham Pharmacia, Piscataway, NJ, USA). Recombinant proteins of each 14-3-3 isoform (0.63 to 10 ng) prepared as described elsewhere⁹ were also subjected to SDS-PAGE and Western blotting as standards. After visualisation with ECL, the densities of the immunoreactive 14-3-3 peaks (optical density (OD) units) were measured with an NIH image analysing system 1.62 (National Institutes of Health, Bethesda, MD, USA) and the levels of total 14-3-3 protein were estimated from the standard curves for the same gel as reported elsewhere.⁹

In 11 patients, neuron-specific enolase (NSE) was measured commercially using an enzyme-linked immunosorbent assay kit (SRL laboratory, Tokyo, Japan) with the same CSF.

3. Results

In seven patients (patients 1 to 7) whose brain MRI scans were normal or showed moderate atrophy, we detected an immunoreactive 30-kDa band against SC-629 (Fig. 1A). In patients 1–6, who had a clear band corresponding to the 14-3-3 protein, the NSE value was more than 25 ng/mL, the cut-off value.¹⁰ However, in patient 7, who had a weak band, the NSE value was 15.8 ng/mL. In the other four patients (patients 8 to 11), whose brain MRI scans indicated very severe brain atrophy, the band was not detected (Fig. 1A). The NSE values of these patients were less than 10 ng/mL. The levels of total 14-3-3 protein in the CSF determined by SC-629 were significantly

Table 1
Profiles of patients enrolled in this study

Patients	1	2	3	4	5	6	7	8	9	10	11
Age/Sex	66/F	74/F	71/M	67/F	55/F	75/F	70/F	79/M	72/F	71/M	74/M
Initial symptom	Head heaviness	Dementia	Dressing apraxia	Diplopia	Somnolence	Ataxia	Ataxia, dementia	Ataxia	General fatigue	Hearing loss	Hallucination
PRNP	ND	ND	M/M	ND	M232R	V/V	ND	V180I	ND	ND	M/M
Myoclonus	+	+	+	+	+	–	+	+	+	+	+
PSWC	+	+	+	+	+	–	+	–	+	+	+
NSE	300	72	25.2	95	110	48	15.8	<10	<10	<10	<10
14-3-3	+	+	+	+	+	+	+	–	–	–	–
Autopsy	ND	+	ND	ND	ND	+	ND	+	ND	ND	+
DL	P	D	P	P	P	D	P	D	P	P	D
Atrophy	Moderate	Slight	Slight	No	No	Slight	Moderate	Severe	Severe	Severe	Severe

F = female, M = Male, PRNP = human prion protein gene, ND = not done, M/M = methionine homozygosity at codon 129 of human prion protein gene, M232R = a point mutation (methionine to arginine) at codon 232 of human prion protein gene, V/V = valine homozygosity at codon 129 of human prion protein gene, V180I = a point mutation (valine to isoleucine) at codon 180 of human prion protein gene, PSWC = periodic sharp wave complexes, NSE = neuron specific enolase in the cerebrospinal fluid (ng/mL), 14-3-3 = 14-3-3 protein in the cerebrospinal fluid; DL = diagnostic level based on WHO criteria; P = probable; D = definite; Atrophy = cerebral atrophy estimated by magnetic resonance imaging.

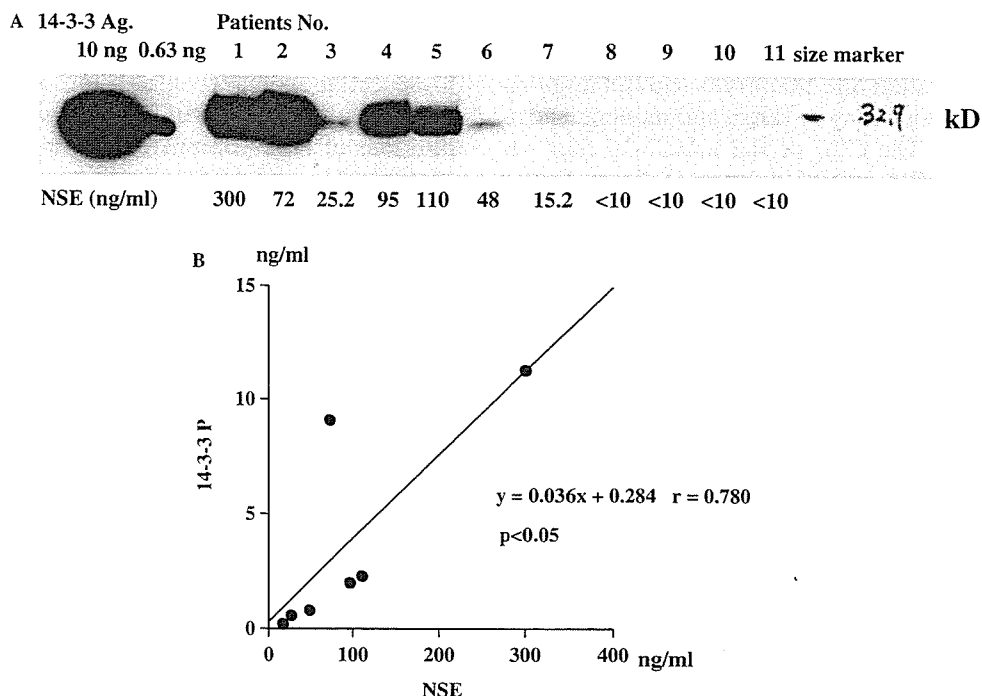


Fig. 1. Detection of 14-3-3 protein in the cerebrospinal fluid (CSF) of Creutzfeldt-Jakob disease (CJD) patients. (A) Western immunoblotting analyses of total 14-3-3 protein in 11 CJD patients using SC-629 antibodies. The levels of neuron-specific enolase (NSE) of these patients were also measured by using an enzyme-linked immunosorbent assay kit. We detected 14-3-3 protein clearly in the CSF of patients 1–6, slightly in patient 7, and not at all in the CSF of patients 8–11. (B) Correlations between the levels of 14-3-3 and those of NSE. The 14-3-3 protein levels in the CSF correlated with those of NSE ($R = 0.780, p < 0.05$).

correlated with those of NSE (Fig. 1B). To analyse the isoform pattern of 14-3-3 in the CSF of the CJD patients, we then evaluated the cross-reactivities of the antibodies we raised and the commercial antibodies against the 14-3-3 isoforms as shown in Fig. 2. The monoclonal antibody for 14-3-3 τ , the polyclonal antibody for η that we raised, and SC-1019 for 14-3-3 ζ were highly specific. The polyclonal antibodies for 14-3-3 γ , ϵ , and β that we prepared were nearly specific except for a slight cross-reaction with 14-3-3 ζ , although commercially available SC-628, SC-732, SC-1020, and SC-731 showed lower isoform specificities (Fig. 2A,B). Based on these results, we analysed the isoform patterns of the CJD patients using the antibodies we

prepared for 14-3-3 β , τ , η , ϵ , and γ , and the commercial SC-1019 for 14-3-3 ζ .

In the six definitely 14-3-3-positive patients (patients 1 to 6), we examined the 14-3-3 isoform patterns (Fig. 3). All patients had an immunoreactive band against 14-3-3 γ , ϵ , ζ , η and β , except for patients 3 and 6, who had a trace immunoreactive band against 14-3-3 η . However, the 14-3-3 τ isoform was not detected in these patients.

4. Discussion

In this study we found that: (1) 14-3-3 protein in the CSF was clearly detected in the progressive stages but

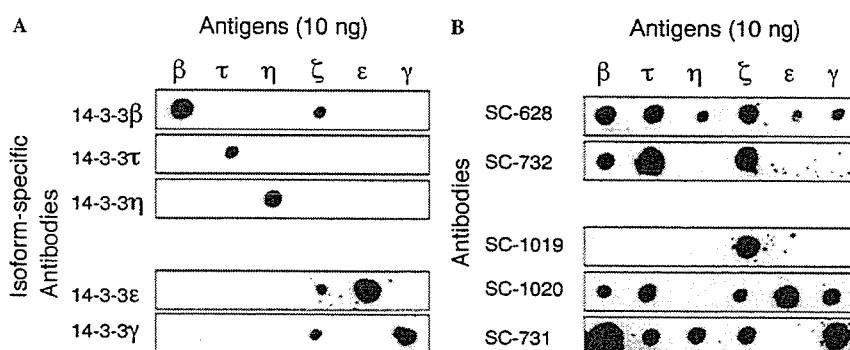


Fig. 2. Specificity of antibodies against 14-3-3 isoforms. (A) The antibodies we raised against 14-3-3 τ and η were highly specific, and those against 14-3-3 γ , ϵ , and β were nearly specific except for a slight cross-reaction with 14-3-3 ζ . These antibodies reacted at a concentration of 2 $\mu\text{g}/\text{mL}$. (B) Among the commercially available antibodies, SC-1019 was highly specific for 14-3-3 ζ , but SC-628, SC-732, SC-1020, and SC-731 demonstrated cross-reactivity with other isoforms. The antibodies reacted at a concentration of 0.2 $\mu\text{g}/\text{mL}$. All commercial antibodies from Santa Cruz Biotechnology, Santa Cruz, CA, USA.

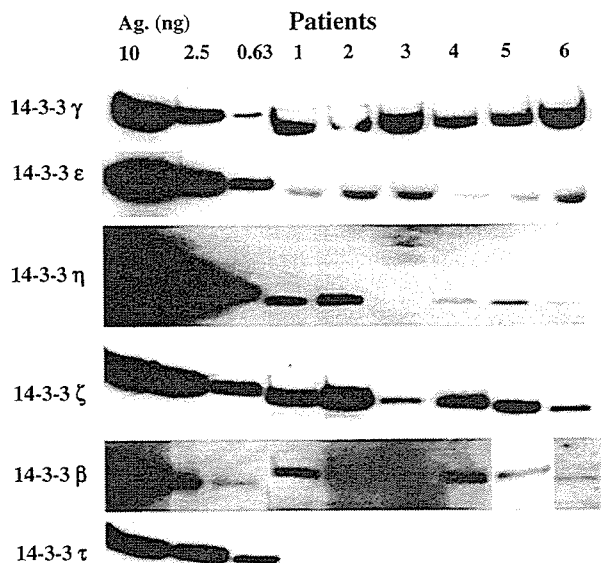


Fig. 3. 14-3-3 isoform patterns in the cerebrospinal fluid of Creutzfeldt-Jakob disease (CJD) patients as detected by Western immunoblotting. The 14-3-3 isoforms of CJD patients 1–6 were detected by the isoform-specific antibodies in Fig. 2A and SC-1019 in Fig. 2B. Each recombinant 14-3-3 isoform protein (0.63–10 ng) was also used as a standard.

not in the terminal stages of the disease, when the brain was severely atrophied; (2) the detected 14-3-3 protein in the CSF of CJD patients comprised five brain-native isoforms; and (3) the levels of 14-3-3 protein in the CSF of CJD patients were correlated with those of NSE, which is a brain-specific protein. These findings reconfirm the fact that 14-3-3 protein is released into the CSF as a consequence of the extensive and rapid destruction of the brain. The detection of five 14-3-3 isoforms, γ , ϵ , η , ζ , and β , may enhance the diagnostic value of 14-3-3 protein in the CSF.

After it was reported that 14-3-3 protein in the CSF is useful for diagnosing CJD,¹ many neurologists studied the protein as a potentially specific marker of CJD. Although 14-3-3 protein is ubiquitously present in almost all tissues, it is particularly abundant in the brain, comprising approximately 1% of the total soluble protein in the brain.¹¹ 14-3-3 protein is essential for cells to survive and acts as an anti-apoptotic protein by regulating protein phosphorylation.¹² 14-3-3 protein with a positive NSE result¹³ was detectable in the CSF in a relatively early phase of CJD, but was under the detection limit in the terminal stage when the brain was severely atrophied. These results suggest that, even in the CSF of typical CJD patients, 14-3-3 protein cannot be detected after neuronal loss is nearly complete. The positive rate of 63.6% (seven of 11) for the 14-3-3 protein immunoassay in the present study was lower than that found in another study.¹⁴ We think the reason for this is that four patients in the terminal stage were included among our 11 patients, not because various subtypes of CJD were included.

In the isoform assay of the CJD patients, we detected five isoforms, 14-3-3 γ , ϵ , η , ζ , and β , but not the τ iso-

form (Fig. 3). 14-3-3 τ is restricted to the hippocampus and medulla oblongata of the mammalian brain, and it is present in very low amounts.⁶ A pathological study showed that the hippocampus and medulla are relatively less affected in CJD, and that T lymphocytes, in which 14-3-3 τ is rich,¹⁵ hardly invade or accumulate in the lesions.¹⁶ These results may support the conclusion that 14-3-3 τ in CSF is under the detection limit. Previously, Van Everbroeck et al. described the detection of 14-3-3 τ by using the antibody SC-732,¹⁷ but this antibody reacts not only with τ but also with β and ζ , as shown in Fig. 2, suggesting that their result may reflect the cross-reaction of SC-732 with the 14-3-3 β and ζ isoforms. The isoform patterns of 14-3-3 protein in the CSF of CJD patients are controversial, and a consensus has not been established yet; γ isoforms,^{1,18} ϵ and γ isoforms,⁷ and β , γ , ϵ , and η isoforms,⁸ partly consistent with our data, have been reported. Based on the results shown in Fig. 2, we speculate that inadequate isoform specificity of the antibodies used may be the cause of the differences in isoform patterns. The great improvements in terms of isoform specificity of the antibodies that we raised may provide more reliable results.

14-3-3 protein is not detected immunologically in the CSF of healthy humans and mammals, and its presence in the CSF suggests leakage of brain cellular proteins due to massive neuronal disruption.¹⁹ Although the detection of 14-3-3 protein in CSF is a sensitive marker for CJD, positive detection has also been reported in other acutely destructive brain diseases, such as cerebrovascular disease, herpes simplex encephalitis, acquired immunodeficiency syndrome (AIDS), malignant brain tumor, hypoxic brain damage, and metabolic encephalopathy.^{1,3,9} Although we did not study the CSF of normal controls because of ethical concerns, we previously reported analyses of 14-3-3 protein, including its isoform pattern, in the CSF of four patients with AIDS dementia complex (ADC), six with cytomegalovirus encephalitis (CMVE), six with cryptococcal meningoencephalitis (CCME), and eight control patients consisting of four with aseptic meningitis, two with amyotrophic lateral sclerosis, one with myasthenia gravis, and one with Parkinson's disease, using the same antibodies as those used in the present study.⁹ The ϵ and γ isoforms were detected in CCME, the ϵ , γ , ζ , and β isoforms were detected in ADC, and the ϵ , γ , and ζ isoforms were detected in CMVE. However, 14-3-3 protein was not detected in the control patients.⁹ The existence of five 14-3-3 isoforms, 14-3-3 γ , ϵ , η , ζ , and β , in the CSF is characteristic of CJD, and detecting the five isoforms is important for a diagnosis of CJD.

Although re-evaluation of the 14-3-3 isoform pattern by using isoform-specific antibodies may still be required, the technique may be useful to differentiate CJD from other diseases, including acutely progressive central nervous system disorders. In addition, the isoform pattern in CJD patients may reflect a difference in the 14-3-3 isoform distribution in the brain.⁶

Acknowledgement

We thank Mr. Brent Bell for reading the manuscript, Dr. Tetsuyuki Kitamoto for analysing the prion protein gene, and Drs Naoshi Okita and Sumireko Sekiguchi for their clinical support. Part of this work was presented at the 125th Annual Meeting of the American Neurological Association, Boston, MA, 17 October 2000. This work was supported by the Slow Virus Infection Research Committee, of the Ministry of Health, Labor and Welfare of Japan.

References

- Zerr I, Bodemer M, Gefeller O, et al. Detection of 14-3-3 protein in the cerebrospinal fluid supports the diagnosis of Creutzfeldt-Jakob disease. *Ann Neurol* 1998;**43**:32–40.
- Zeidler M, Gibbs Jr CJ, Meslin F. *WHO Manual for Strengthening Diagnosis and Surveillance of Creutzfeldt-Jakob Disease*. Geneva: WHO; 1998.
- Huang N, Marie SK, Livramento JA, et al. 14-3-3 protein in the CSF of patients with rapidly progressive dementia. *Neurology* 2003;**61**:354–7.
- Chapman T, McKeel Jr DW, Morris JC. Misleading results with the 14-3-3 assay for the diagnosis of Creutzfeldt-Jakob disease. *Neurology* 2000;**55**:1396–7.
- Leffers H, Madsen P, Rasmussen HH, et al. Molecular cloning and expression of the transformation sensitive epithelial marker stratifin. A member of a protein family that has been involved in the protein kinase C signalling pathway. *J Mol Biol* 1993;**20**:982–98.
- Baxter HC, Liu WG, Forster JL, et al. Immunolocalisation of 14-3-3 isoforms in normal and scrapie-infected murine brain. *Neuroscience* 2002;**109**:5–14.
- Takahashi H, Iwata T, Kitagawa Y, et al. Increased levels of ϵ and γ isoforms of 14-3-3 proteins in cerebrospinal fluid in patients with Creutzfeldt-Jakob disease. *Clin Diagn Lab Immunol* 1999;**6**:983–5.
- Wiltfang J, Otto M, Baxter HC, et al. Isoform pattern of 14-3-3 proteins in the cerebrospinal fluid of patients with Creutzfeldt-Jakob disease. *J Neurochem* 1999;**73**:2485–90.
- Wakabayashi H, Yano M, Tachikawa N, et al. Increased concentrations of 14-3-3 ϵ , γ and ζ isoforms in cerebrospinal fluid of AIDS patients with neuronal destruction. *Clinica Chimica Acta* 2001;**312**:97–105.
- Beaudry P, Cohen P, Brandel PJ, et al. 14-3-3 protein, neuron-specific enolase, and S-100 protein in cerebrospinal fluid of patients with Creutzfeldt-Jakob disease. *Dement Geriatr Cogn Disord* 1999;**10**:40–6.
- Boston PF, Jackson P, Thompson RJ. Human 14-3-3 protein: radioimmunoassay, tissue disturbance, and cerebrospinal fluid levels in patients with neurological disorders. *J Neurochem* 1982;**38**:1475–82.
- Wang HG, Pathan N, Ethell IM, et al. Ca^{2+} -induced apoptosis through calcineurin dephosphorylation of BAD. *Science* 1999;**284**:339–43.
- Zerr I, Bodemer M, R acker S, et al. Cerebrospinal fluid concentration of neuron-specific enolase in diagnosis of Creutzfeldt-Jakob disease. *Lancet* 1995;**345**:1609–10.
- Shiga Y, Miyazawa K, Sato S, et al. Diffusion-weighted MRI abnormalities as an early diagnostic marker for Creutzfeldt-Jakob disease. *Neurology* 2004;**63**:443–9.
- Meller N, Liu YC, Collins TL, et al. Direct interaction between protein kinase C θ PKC θ and 14-3-3 t in T cells: 14-3-3 overexpression results in inhibition of PKC θ translocation and function. *Mol Cell Biol* 1996;**16**:5782–91.
- S anchez-Valle R, Saiz A, Graus F. 14-3-3 protein isoforms and atypical patterns of the 14-3-3 assay in the diagnosis of Creutzfeldt-Jakob disease. *Neurosci Lett* 2002;**320**:69–72.
- Van Everbroeck BRJ, Boons J, Cras P. 14-3-3 γ -isoform detection distinguishes sporadic Creutzfeldt-Jakob disease from other dementias. *J Neurol Neurosurg Psychiatry* 2005;**76**:100–2.
- Hsich G, Kenney K, Gibbs CJ, et al. The 14-3-3 brain protein in cerebrospinal fluid as a marker for transmissible spongiform encephalopathies. *N Engl J Med* 1996;**335**:924–30.
- Lemstra AW, van Meejen MT, Vreyling JP, et al. 14-3-3 testing in diagnosing Creutzfeldt-Jakob disease: a prospective study in 112 patients. *Neurology* 2000;**55**:514–6.

Prion Strain-Dependent Differences in Conversion of Mutant Prion Proteins in Cell Culture

Ryuichiro Atarashi,^{1,2*} Valerie L. Sim,² Noriyuki Nishida,¹ Byron Caughey,² and Shigeru Katamine¹

Department of Molecular Microbiology and Immunology, Nagasaki University Graduate School of Biomedical Sciences, 1-12-4 Sakamoto, Nagasaki 853-8523, Japan,¹ and Laboratory of Persistent Viral Diseases, Rocky Mountain Laboratories, National Institute of Allergy and Infectious Diseases, National Institutes of Health, Hamilton, Montana 59840²

Received 28 February 2006/Accepted 19 May 2006

Although the protein-only hypothesis proposes that it is the conformation of abnormal prion protein (PrP^{Sc}) that determines strain diversity, the molecular basis of strains remains to be elucidated. In the present study, we generated a series of mutations in the normal prion protein (PrP^C) in which a single glutamine residue was replaced with a basic amino acid and compared their abilities to convert to PrP^{Sc} in cultured neuronal N2a58 cells infected with either the Chandler or 22L mouse-adapted scrapie strain. In mice, these strains generate PrP^{Sc} of the same sequence but different conformations, as judged by infrared spectroscopy. Substitutions at codons 97, 167, 171, and 216 generated PrP^C that resisted conversion and inhibited the conversion of coexpressed wild-type PrP in both Chandler-infected and 22L-infected cells. Interestingly, substitutions at codons 185 and 218 gave strain-dependent effects. The Q185R and Q185K PrP were efficiently converted to PrP^{Sc} in Chandler-infected but not 22L-infected cells. Conversely, Q218R and Q218H PrP were converted only in 22L-infected cells. Moreover, the Q218K PrP exerted a potent inhibitory effect on the conversion of coexpressed wild-type PrP in Chandler-infected cells but had little effect on 22L-infected cells. These results show that two strains with the same PrP sequence but different conformations have differing abilities to convert the same mutated PrP^C.

Transmissible spongiform encephalopathies (TSE), or prion diseases, are lethal neurodegenerative diseases that include Creutzfeldt-Jakob disease in humans, scrapie in sheep, and bovine spongiform encephalopathy in cattle. The infectious agent, termed prion, is unique in that no agent-specific nucleic acid is detectable. The protein-only hypothesis proposes that this agent consists solely of an abnormal form of prion protein (PrP^{Sc}), which is produced by the conversion of the normal cellular prion protein (PrP^C) and accumulates primarily in the lymphoreticular and central nervous system during the course of prion disease (41, 56). PrP^C, a host-encoded glycoprotein anchored to the cell membrane by a glycosyl-phosphatidylinositol moiety, is expressed mainly in the central nervous system. PrP^C is detergent soluble and proteinase K (PK) sensitive, whereas PrP^{Sc} is detergent insoluble and partially PK resistant (35). These different biophysical properties are thought to be due to different conformations of the two isoforms. PrP^C is highly α -helical, but PrP^{Sc} has a large proportion of β -sheet structure (14, 38).

Various TSE strains with distinct biological characteristics have been identified in several mammalian species. These strains are characterized by different incubation periods and histopathological changes (9, 10). Generally, the phenotypic characteristics are maintained upon repeated passages in the same species with the same PrP amino acid sequence. In addition, previous reports showed that strain-specific biological characteristics remain unchanged after passages in cell cultures (2, 8). In contrast, changing to a species with a different PrP

sequence often results in the emergence of a new strain (28, 29). The existence of multiple strains signifies that the infectious agent carries some form of strain-specific information that determines each strain's characteristics. One possibility is that this information stems from the distinct PrP^{Sc} conformation of each strain. Differences in the electrophoretic mobilities of PK-resistant PrP^{Sc} core fragments among strains are well documented (7, 16, 50). These different-sized PrP^{Sc} fragments are likely a consequence of differing conformations and thus different PK cleavage points. Conformational differences in β -sheet structures between strains have also been demonstrated by infrared (IR) spectroscopy (13, 52). Furthermore, Syrian hamster (SHa) PrP^{Sc}, when denatured, binds more anti-PrP antibody than when it is in its native form, and each strain can have distinct denatured versus nondenatured binding ratios (44). In addition, some Syrian hamster TSE strains are reported to differ in the extent of their PK resistance after partial denaturation with guanidine hydrochloride (39). These findings support the hypothesis that TSE strains have distinct PrP^{Sc} conformations. Moreover, cell-free conversion experiments have shown that different forms of PrP^{Sc} can induce strain-specific conformational changes in PrP^C (6), and Jones and Surewicz recently reported that artificial amyloid fibrils of PrP23-144 from different species revealed strain-like behavior in vitro (25). Nevertheless, much remains to be learned about the mechanistic relationship between PrP^{Sc} conformational differences and the molecular basis of TSE strains.

Studies using transgenic mice and congenic mice have shown that several TSE strains differ in incubation periods in the same host (11, 23, 32). The molecular basis of this remains unresolved, but the conformation of PrP^{Sc} could influence incubation periods by affecting the efficiency and location of

* Corresponding author. Mailing address: Laboratory of Persistent Viral Diseases, Rocky Mountain Laboratories, NIAID, NIH, 903 South 4th Street, Hamilton, MT 59840. Phone: (406) 363-9341. Fax: (406) 363-9286. E-mail: atarashir@niaid.nih.gov.

PrP^{Sc} formation. However, to date, there are little data on the influence of PrP mutations on PrP^{Sc} formation *in vitro*.

Because N2a58 cells overexpressing mouse PrP can be persistently infected with the Chandler or 22L prion strain (37), we chose to examine the strain-specific effect of PrP mutations on PrP^{Sc} formation in N2a58 cell cultures infected with the Chandler or 22L strain, designated Ch-N2a58 and 22L-N2a58, respectively. Although little is known about which amino acid residues of the PrP sequence correlate with the strain-specific formation of PrP^{Sc}, we noticed that mutations from glutamine to arginine or lysine in the C terminus of the PrP were related to the resistance of prion diseases (4, 47, 57) and inhibited the conversion of coexpressed wild-type PrP in Chandler-infected N2a cell cultures (26). In this study, we created a series of PrP mutations in which a single glutamine residue was replaced with an arginine residue and compared the effects of these mutations on PrP^{Sc} formation in Ch- and 22L-N2a58 cells. We demonstrated that specific amino acids residues in PrP^C can allow or inhibit PrP^{Sc} formation *in vitro* for one strain but not another even though the amino acid sequence of PrP^{Sc} is the same in each strain. Our results suggest that each prion strain can interact with PrP^C in a strain-specific manner, producing PrP^{Sc} with a strain-specific conformation and unique biological characteristics.

MATERIALS AND METHODS

Cell culture. N2a58 cells overexpressing mouse PrP (PrP-a genotype, codons 108L and 189T) were prepared as described previously (37). To create N2a58 cells infected with either the Chandler/RML or 22L strain (Ch-N2a58 and 22L-N2a58), the cells were incubated with brain homogenates from ddY mice infected with each strain. After subcloning by limiting dilution, several PrP^{Sc}-positive clones were isolated. The cell clones producing the highest level of PrP^{Sc} were used for subsequent study. Both Ch-N2a58 and 22L-N2a58 cells stably expressed PrP^{Sc} for over 50 passages. Morphological appearances and growth characteristics of these prion-infected cells were indistinguishable from those of N2a58 cells (data not shown). All cells were cultured in Opti-MEM (Invitrogen) containing 10% fetal bovine serum and penicillin-streptomycin at 37°C in 5% CO₂ and were split every 3 to 4 days at an 8- to 10-fold dilution.

Plasmid constructions. The open reading frames of Syrian hamster PrP (SHa), human PrP (Hu), and mouse PrP containing the epitope for the 3F4 antibody (Mo3F4) were amplified by PCR with mouse DNA, MHM2/Mo3F4 PrP transgenic mouse DNA, SHa PrP transgenic mouse (3) DNA, and human DNA, respectively. Amplified fragments were inserted into the pcDNA3.1(+) vector (Invitrogen) between the BamHI and XbaI sites. Mouse PrP (PrP-a genotype) containing the epitope for the L42 antibody (MoL42) was introduced into mouse PrP by PCR-direct mutagenesis.

Mo3F4 PrP differs from the mouse PrP-a genotype by two amino acids, L108M and V111M, which are included in the epitope recognized by the 3F4 anti-PrP monoclonal antibody (Dako). MoL42 PrP has one amino acid substitution, W144Y, which is recognized by the L42 anti-PrP antibody (R-biopharm) (54). Since neither antibody reacts with mouse PrP, transfected recombinant PrP is distinguishable from endogenous mouse PrP.

Mo3F4 sequences with specific amino acid changes (Q90R, Q97R, Q159R, Q167R, Q171R, Q185R, Q185K, Q185H, Q185E, Q185L, Q211R, Q216R, Q218R, Q218K, Q218H, Q218E, Q218L, and Q222R) were generated by PCR mutagenesis. The resulting PCR fragments were subcloned into the pcDNA3.1(+) vector. To create MoL42 mutations with specific amino acid changes (Q185R, Q218R, Q218K, and Q218H), BamHI-BstPI fragments of the corresponding Mo3F4 mutants in the pcDNA3.1(+) vector were replaced by those of MoL42 PrP. The PrP sequences of all plasmids used in this study were confirmed by using the ABI PRISM 3100 genetic analyzer (Applied Biosystems), and no unexpected mutations were found.

Transfection and Western blotting. N2a58, Ch-N2a58, and 22L-N2a58 cells were transiently transfected with various plasmid constructs (1 or 2 µg DNA per 6-cm dish) using the Effectene transfection reagent (QIAGEN) according to the manufacturer's instructions. To evaluate dominant-negative inhibition of PrP^{Sc} formation, cotransfections of two different PrP constructs were performed with

a DNA ratio of 1:1 or 1:2. Indirect immunofluorescence of PrP and fluorescence imaging of pEGFP-C1 (Clontech) revealed that transfection efficiencies were around 40 to 60% and that the rate of the overlapping expression of two plasmids cotransfected was more than 90%.

After 72 h of transfection, cells from a 6-cm dish were lysed in 0.5 ml of lysis buffer (150 mM NaCl, 50 mM Tris-HCl [pH 7.5], 0.5% Triton X-100, 0.5% sodium deoxycholate, and 1 mM EDTA). After cell debris and nuclei were removed by low-speed centrifugation, the protein concentration of the supernatant was measured by the BCA protein assay (Pierce). To detect PrP^{Sc}, the protein concentration of the supernatant was adjusted with lysis buffer to 1 mg/ml. Samples of equal protein concentrations and volumes were digested with 20 µg/ml of proteinase K at 37°C for 45 min, and the digestion was stopped by adding phenylmethylsulfonyl fluoride (2 mM). After 60 min of centrifugation at 20,400 × g, the pellet was dissolved with sample buffer (4 M urea, 4% sodium dodecyl sulfate, 100 mM dithiothreitol, 10% glycerol, 0.02% bromophenol blue, and 50 mM Tris-HCl [pH 6.8]), boiled, and then loaded onto a 15% polyacrylamide gel. Proteins were transferred onto a membrane (Immobilon P; Millipore). 3F4-positive PrPs were detected with 3F4 antibody, L42-positive PrPs were detected with L42 antibody, and total PrP was detected with mouse polyclonal anti-PrP antibody (designated SS). Immunoreactive bands were visualized using the ECL detection system (Amersham Biosciences). The expression level of transfected PrP in cell lysates (30 µg of total protein per lane) was also estimated by immunoblotting. Densitometric analysis of the film was performed using NIH Image software. The conversion efficiency of Mo3F4 was assigned as 100%, and the level of PrP^{Sc} formation in each 3F4-positive mutant was calculated relative to this value. In some experiments, the cell lysates with proteinase K treatment were digested with PNGase F (New England Biolabs).

IR spectroscopy of PrP^{Sc}. PrP^{Sc} was isolated from the brains of mice affected by either 22L, Chandler, or 87V scrapie and treated with PK as described previously (13). For IR analysis, ~3 µl of pelleted slurries containing at least 10 mg/ml PrP^{Sc} in a solution containing 20 mM sodium phosphate, 130 mM NaCl (pH 7.5), and 0.5% sulfobetaine was applied to a Golden Gate Single Reflection Diamond Attenuated Total Reflectance unit purged with dry air and covered to prevent sample evaporation. Data collection was performed using a System 2000 IR instrument (Perkin-Elmer). Test conditions were as follows: 20°C, 4.00-cm⁻¹ resolution, 2-cm/s optical path difference velocity, 1,000 scans, and 0.5-cm⁻¹ data interval. The detector was an nb1 MCT detector cooled by liquid nitrogen. Primary spectra were obtained by subtracting the spectra of the corresponding buffer or buffer with additives and water vapor and by adjusting the baseline and normalizing for comparable absorbance of different concentrations of PrP. Second-derivative spectra were calculated from the primary spectra using 13 data points. The software used for spectral analyses was Spectrum v2.00 (Perkin-Elmer).

RESULTS

Mo3F4 PrP converts to PrP^{Sc} with similar efficiency in Ch-N2a58 and 22L-N2a58 cells. Prior to creating PrP mutants, we first confirmed that our starting Mo3F4 vector could convert to PrP^{Sc} in cells persistently infected with the Chandler or 22L mouse-adapted scrapie strain (Ch-N2a58 and 22L-N2a58 cells, respectively). The presence of endogenous mouse PrP^{Sc} in the Ch-N2a58 and 22L-N2a58 cells was confirmed by immunoblotting with the mouse polyclonal anti-PrP SS antibody. Similar amounts of endogenous mouse PrP^{Sc} accumulated in Ch-N2a58 and 22L-N2a58 cells, while none was detected in uninfected N2a58 cells (Fig. 1A). In the transfected cells, PK-resistant PrP^{Sc} derived from Mo3F4 PrP was distinguished from endogenous mouse PrP^{Sc} by immunoblotting with the monoclonal anti-PrP 3F4 antibody (Fig. 1B). PK-resistant PrP^{Sc} core fragments from Ch-N2a58 and 22L-N2a58 cells were treated with PNGase F to remove asparagine-linked glycosylation and immunoblotted with either SS or 3F4 antibody. No differences in gel migration patterns were seen (Fig. 1C).

Q218K PrP does not convert and inhibits PrP^{Sc} formation from coexpressed Mo3F4 PrP in Ch-N2a58 but not in 22L-N2a58 cells. In order to compare the consequences of changes in the PrP primary structure between Ch-N2a58 and 22L-

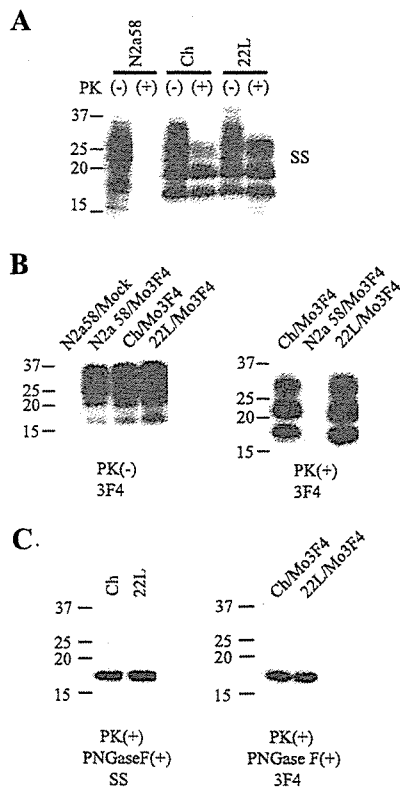


FIG. 1. Formation of Mo3F4-derived PrP^{Sc} in Ch-N2a58 and 22L-N2a58 cells. (A) Western blot using polyclonal anti-PrP antibody SS in N2a58, Ch-N2a58 (Ch), and 22L-N2a58 (22L) cells without (-) or with (+) PK treatment. (B) Expression levels of Mo3F4 PrP (left panel) and detection of Mo3F4-derived PrP^{Sc} (right panel) were measured by Western blot using monoclonal antibody 3F4. Mock, untransfected cells. (C) After consecutive treatments of PK and PNGase F, untransfected (left panel) and Mo3F4 PrP-transfected cells (right panel) were analyzed by Western blotting using SS and 3F4 antibodies, respectively. Molecular mass markers are indicated in kilodaltons on the left side of each panel.

N2a58 cells, we first examined the PrP^{Sc} formation of two heterologous PrPs, Syrian hamster (SHa) and human (Hu) PrPs, and two Mo3F4 mutated PrPs with a single amino acid substitution at codon 218, Q218K and Q218E, in the infected cells transfected with the corresponding expression vectors. The 3F4 antibody detected SHa, Hu, and Mo3F4 mutated PrPs expressed in Ch-N2a58 and 22L-N2a58 cells at a level similar to that of wild-type Mo3F4 PrP (Fig. 2A, lower panels). SHa, Hu, Q218K, and Q218E PrP did not convert to PrP^{Sc} in Ch-N2a58 (Fig. 2A, upper panel, lanes 3 to 6) and 22L-N2a58 (Fig. 2A, upper panel, lanes 9 to 12) cells.

To evaluate the inhibitory effect of these heterologous and mutated PrPs, each expression vector was cotransfected with that of Mo3F4 PrP at a DNA ratio of 1:1 or 1:2. As seen previously (26), in Ch-N2a58 cells, Q218K PrP completely inhibited the accumulation of PrP^{Sc} derived from Mo3F4 PrP even at a DNA ratio of 1:1 (Fig. 2B, upper panel, lanes 8 and 9). SHa, Hu, and Q218E PrP also revealed a dose-dependent inhibitory effect but to a lesser extent (Fig. 2B, upper panel, lanes 3 to 6, 10, and 11). In remarkable contrast, in 22L-N2a58

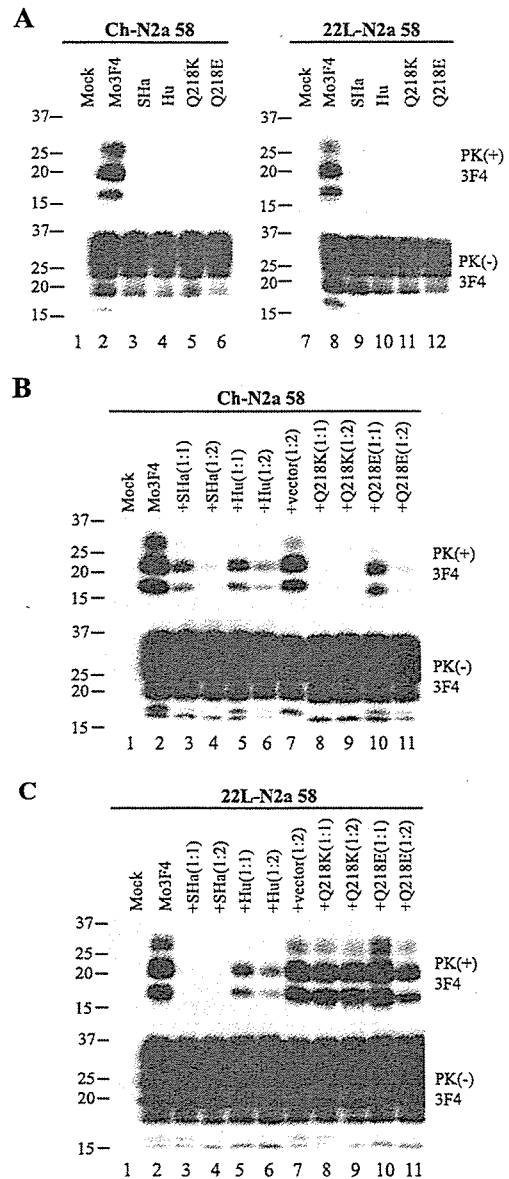


FIG. 2. Strain-dependent inhibitory effect of Q218K mutation on PrP^{Sc} formation of wild-type Mo3F4. (A) Conversion to 3F4-positive PrP^{Sc} (upper panels) and expression of Mo3F4, SHa, Hu, Q218K, and Q218E (lower panels) were measured by Western blot using 3F4 antibody. The 3F4 epitope was present in all these constructs. (B and C) The inhibitory effect of the constructs was determined by cotransfection with Mo3F4 in the DNA ratio of 1:1 or 1:2. The blots were probed with 3F4 antibody. Mock, untransfected cells; +vector(1:2), cotransfection of Mo3F4 and pcDNA3.1(+) at a 1:2 ratio.

cells, Q218K PrP had little effect on Mo3F4 PrP^{Sc} accumulation (Fig. 2C, upper panel, lanes 8 and 9). The inhibitory effect of Q218E PrP in 22L-N2a58 cells was also very weak (Fig. 2C, upper panel, lanes 10 and 11). Conversely, SHa PrP inhibited Mo3F4-derived PrP^{Sc} formation to a greater extent in 22L-N2a58 cells than in Ch-N2a58 cells (Fig. 2C, upper panel, lanes 3 and 4). These results were reproduced in three independent experiments (Table 1). These data suggest that the inhibition

TABLE 1. Summary of results

Mutations	Chandler		22L	
	Conversion ^a	Inhibition ^b	Conversion ^a	Inhibition ^b
SHa	-	+	-	2+
Hu	-	+	-	+
Q90R	+	NA	+	NA
Q97R	-	2+	-	2+
Q159R	+	NA	+	NA
Q167R	-	2+	-	+
Q171R	-	2+	-	2+
Q185R	+	NA	-	2+
Q185K	2+	NA	-	2+
Q185H	+	NA	+/-	+
Q185E	-	+	-	+/-
Q185L	+/-	+	+/-	+
Q211R	+	NA	+	NA
Q216R	-	+	-	2+
Q218R	-	2+	+	NA
Q218K	-	2+	-	-
Q218H	-	2+	+	NA
Q218E	-	+	+/-	-
Q218L	+/-	+	+	NA
Q222R	+	NA	+	NA

^a PrP^{Sc} formation of each 3F4-positive construct was quantified by densitometric analysis. The percent conversion of Mo3F4 was assigned as 100%, and the relative scores compared with Mo3F4 are shown. 2+ indicates >200%; + indicates 50 to 200%; +/- indicates 10 to 50%; - indicates <10%. Each value represents the mean of two or three replicates.

^b Relative inhibitory effect on PrP^{Sc} formation of conversion-defective mutated PrPs was assessed. 2+ indicates >80% inhibition of Mo3F4 PrP^{Sc} formation (in the DNA ratio of 1:1); + indicates 50 to 80% inhibition (1:1); +/- indicates <50% inhibition (1:1) and >50% inhibition (1:2); - indicates <50% inhibition (1:1 and 1:2). Each value represents the mean of two or three replicates. NA, not applicable.

of PrP^{Sc} formation by some of these PrP molecules, especially Q218K, is strain specific.

Q185R PrP converts to PrP^{Sc} in Ch-N2a58 but not 22L-N2a58 cells. To further analyze the strain-specific effect of PrP mutations on PrP^{Sc} formation in Ch-N2a58 and 22L-N2a58 cells, we generated nine 3F4-positive mutated PrPs with a single arginine substitution for each glutamine residue in the C-terminal half and examined their conversion efficiencies in the infected cells (see Fig. 6). The Q90R, Q159R, Q211R, and Q222R PrPs readily converted to PrP^{Sc} in Ch-N2a58 and 22L-N2a58 cells (Fig. 3A, upper panels), whereas the Q97R, Q167R, Q171R, and Q216R PrPs failed to convert in both cell lines (Fig. 3A, upper panels). These conversion-defective mutated PrPs potentially inhibited the accumulation of wild-type Mo3F4-derived PrP^{Sc} in both cell lines (Fig. 3B, upper panels). Interestingly, Q185R PrP efficiently converted in Ch-N2a58 cells but not in 22L-N2a58 cells (Fig. 3A), where it actually had an inhibitory effect (Fig. 3B, upper panel, and Table 1).

Substitutions of various amino acid species at codons 185 and 218 differentially affect PrP^{Sc} formation between Ch- and 22L-N2a58 cells. To further examine the effect of amino acid substitutions at codons 185 and 218, where strain-specific effects were observed, we replaced each glutamine residue (Q) with various amino acid species, including basic amino acids (R, K, and H), an acidic amino acid (E), and a hydrophobic amino acid (L). As shown in Fig. 4A and Table 1, Q185K, Q185H, and Q185R PrP readily converted to PrP^{Sc} in Ch-N2a58 cells. Interestingly, the amount of Q185K-derived PrP^{Sc}

accumulation in Ch-N2a58 cells was higher than that of Mo3F4-derived PrP^{Sc}, suggesting a more efficient conversion of these mutated PrPs in the cells. In contrast, in 22L-N2a58 cells, little PrP^{Sc} derived from Q185R, Q185K, and Q185H PrP accumulated. Q185E and Q185L PrP minimally converted to PrP^{Sc} in both Ch- and 22L-N2a58 cells.

The introduction of substitutions at codon 218, including basic amino acids (R, K, and H), resulted in the loss of conversion in Ch-N2a58 cells (Fig. 4B). Conversely, in 22L-N2a58 cells, Q218R, Q218H, and Q218L efficiently converted to PrP^{Sc}. Q218K PrP did not convert in either cell line (Fig. 4B) and failed to inhibit wild-type Mo3F4 PrP^{Sc} formation (Fig. 2C).

To determine whether different cellular localizations of the mutated PrPs might be the cause of the different conversion effects, we examined the mutated PrPs with indirect immunofluorescence using the 3F4 antibody. Mo3F4, Q185R, Q218R, and Q218K all localized to the cell surface of Ch-N2a58 and 22L-N2a58 cells (data not shown). In addition, phosphatidylinositol-specific phospholipase C treatment removed the mutated PrPs from the cell surface (data not shown). These results demonstrate that the localization of the mutated PrPs cannot account for their strain-specific properties.

Strain-specific properties of the PrP mutations are independent of antibody epitopes. To assess whether the 3F4 epitope can influence the strain-specific properties of the mutated PrPs, we replaced the 3F4 epitope with the L42 epitope (W144Y), because others have previously shown that MoL42 PrP, like Mo3F4 PrP, readily converted to PrP^{Sc} in ScN2a cells (55). Expression of the L42-positive PrPs, MoL42, Q185R, Q218H, Q218R, and Q218K PrPs, was confirmed by Western blotting using the L42 antibody (Fig. 5A, lower panels). The conversion efficiencies of these L42-positive mutated PrPs were similar to those of 3F4-positive mutated PrPs (Fig. 5A, upper panels). Moreover, as shown in Fig. 5B, Q218K PrP again showed strain-dependent effects on MoL42-derived PrP^{Sc}. The data shown in Fig. 5 indicate that changing from a 3F4 epitope to an L42 epitope in the mutant PrPs does not significantly affect their strain-specific effects on PrP^{Sc} formation.

22L and Chandler PrP^{Sc} have different conformations by IR spectra. To assess whether there are any detectable differences in structure between 22L and Chandler PrP^{Sc}, we performed IR spectroscopy. The amide I region (1,600 to 1,700 cm⁻¹) of protein IR spectra is sensitive to differences in protein secondary structure. Although it is difficult to make complete and unequivocal assignments of IR amide I bands, predominantly α -helical and β -sheet proteins have absorption maxima of 1,653 to 1,657 cm⁻¹ and 1,615 to 1,640 cm⁻¹, respectively, in water-based (as opposed to D₂O-based) media (see Fig. 7). Unfolded or random-coil polypeptides tend to have absorbance maxima near 1,645 to 1,650 cm⁻¹, and turn structures tend to absorb between 1,660 and 1,680 cm⁻¹. Absorbance maxima are represented by negative deflections in the second-derivative spectra shown in Fig. 7. Previous studies have shown that the infrared spectrum of PrP^{Sc} of different hamster TSE strains can vary markedly despite being composed of PrP molecules of the same amino acid sequence (13, 52). Consistent with that theme, PK-treated PrP^{Sc} isolated from the brains of mice with 22L and Chandler scrapie differed in the IR spectral

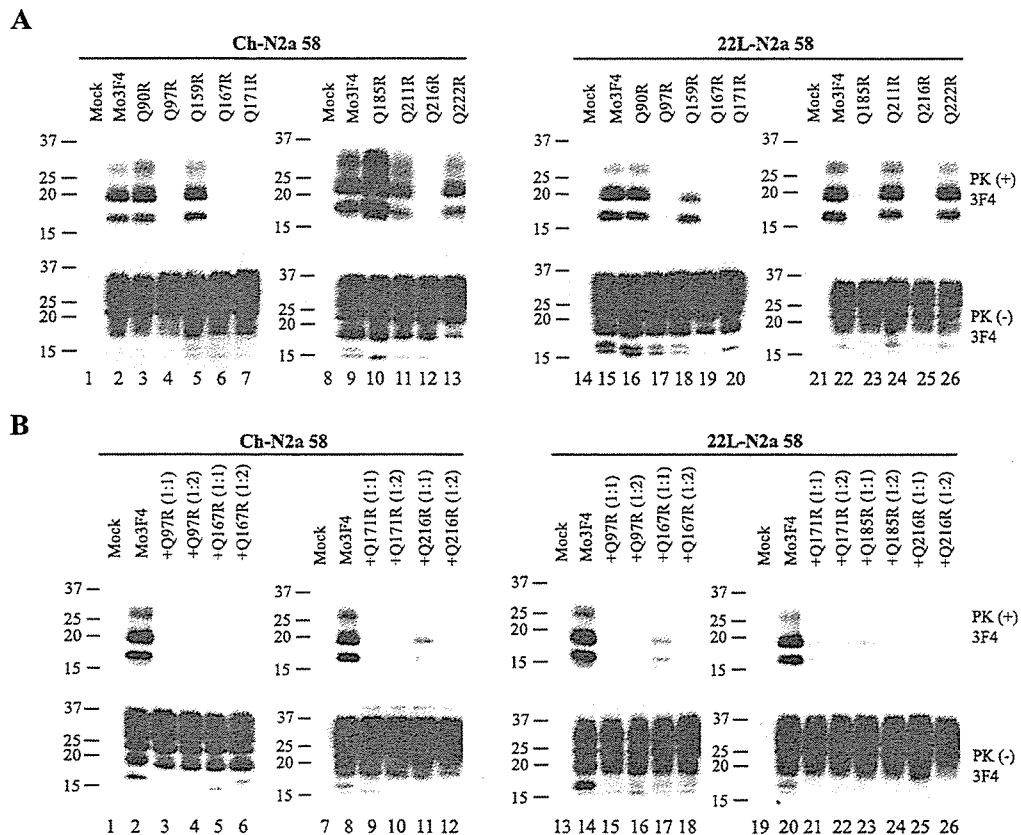


FIG. 3. Strain-specific effects of Q185R mutation on PrP^{Sc} formation. (A) Conversion to 3F4-positive PrP^{Sc} (upper panels) and expression of Mo3F4, Q90R, Q97R, Q159R, Q167R, Q171R, Q185R, Q211R, Q216R, and Q222R (lower panels) were measured by Western blotting using 3F4 antibody. The 3F4 epitope was present in all these constructs. (B) Inhibitory effects of constructs that did not convert were determined by cotransfection with Mo3F4 at a 1:1 or 1:2 DNA ratio. The blots were probed with 3F4 antibody.

region commonly ascribed to the β -sheet region (see Fig. 7). For comparison, PrP^{Sc} from another mouse scrapie strain, 87V, is also shown to have a distinct infrared spectrum in the β -sheet region. In contrast, hemoglobin, a highly α -helical protein, has very little absorbance in the β -sheet region. These results provide direct spectroscopic evidence for differences in conformation between 22L, Chandler, and 87V PrP^{Sc}.

DISCUSSION

In this study, we found evidence that TSE strain characteristics depend on their conformation. We showed that substitutions at codons 185 and 218 resulted in strain-specific PrP^{Sc} formation in cultured neuronal cells infected with two mouse-adapted scrapie prion strains, Chandler and 22L. While others previously demonstrated conformational differences between strains (13, 39, 44, 52), and some strain-specific differences in conformation have been observed in cell-free conversions (6), synthetic amyloid fibrils (25), and purified recombinant *Saccharomyces cerevisiae* Sup35 (31, 49), our results are the first to be obtained from a cell culture comparison of strain effects on the conversion of a panel of mutant PrP^c molecules.

The amino acid sequence of PrP can certainly influence the efficiency of transmission of the infectious agent to a new host

species (45), but this "species barrier" cannot be explained on the basis of sequence heterogeneity alone. Our results demonstrate that TSE strains with the same sequence have various abilities to convert the PrP^c mutants at codons 185 and 218, implying a sequence-independent cause of strain specificity. Although the most efficient conversions are expected to occur between PrP^c and PrP^{Sc} with identical sequences, our Q185K mutation promoted PrP^{Sc} formation in CH-N2a58 cells at a rate higher than that of the homologous wild-type PrP^c (Table 1), indicating that sequence homology between PrP^c and PrP^{Sc} does not necessarily guarantee the most efficient PrP^{Sc} formation.

The locations of residues 185 and 218 within the secondary structure of PrP may explain why mutations at these sites revealed strain-specific differences in conversion. The nuclear magnetic resonance structure of mouse PrP contains three α -helices comprised of residues 144 to 154, 175 to 193, and 200 to 219; two β -strands containing residues 128 to 131 and 161 to 164; and a disulfide bridge between C178 and C213, linking helices 2 and 3 (42). Amino acid 185 is in helix 2, and residue 218 is in the C-terminal portion of helix 3 (Fig. 6). Helices 2 and 3 and their disulfide bridge are crucial for PrP^{Sc} formation (22, 36), and many point mutations associated with familial human prion diseases are located within or adjacent to these

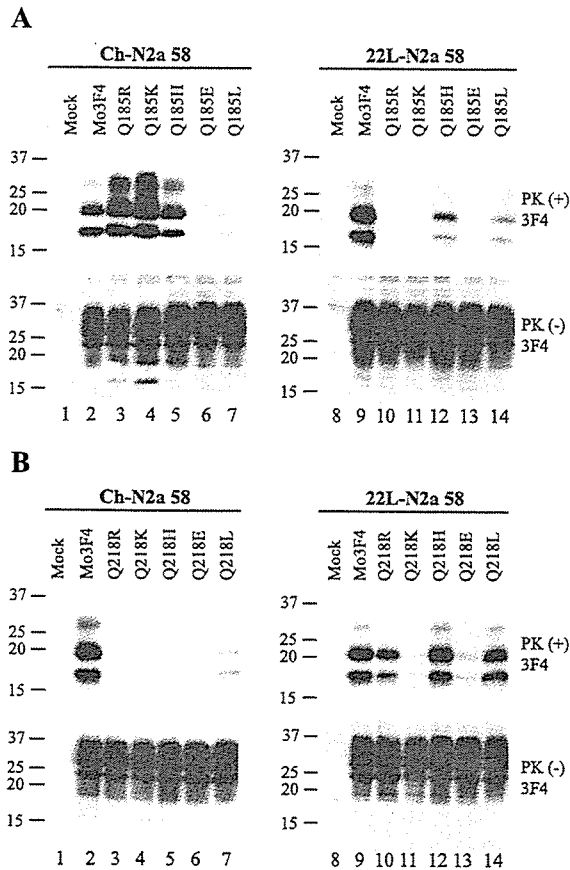


FIG. 4. Strain-specific PrP^{Sc} formation of Q185R, Q185K, Q218R, and Q218H mutated PrP. (A) Conversion to 3F4-positive PrP^{Sc} (upper panels) and expression of Mo3F4, Q185R, Q185K, Q185H, Q185E, and Q185L (lower panels) were measured by Western blot using 3F4 antibody. The 3F4 epitope was present in all these constructs. (B) Western blotting of Mo3F4, Q218R, Q218K, Q218H, Q218E, and Q218L was done as in A.

two helices (41). One such mutation, D178N, is seen in two clinicopathologically distinct diseases, fatal familial insomnia and Creutzfeldt-Jakob disease, the phenotype being determined by the methionine-valine polymorphism at codon 129 on the D178N mutation phenotype suggests that there may be a modifiable electrostatic interaction or hydrogen bonding between residues 129 and 178 in human PrP (1, 43). Of note, anti-PrP antibody binding studies have revealed that the main conformational differences between PrP^c and PrP^{Sc} actually lie toward the N-terminal region in residues 90 to 120, while the C-terminal regions, including helices 2 and 3, remain accessible to antibody in both forms of PrP, implying that their conformation is not significantly altered during conversion (40). This is also consistent with the maintenance of significant α -helical secondary structure content in PrP^{Sc} (13, 14, 38). In addition, a conformation-dependent immunoassay has localized the primary structural differences among PrP^{Sc} strains to their N termini (44). Such observations suggest that helices 2 and 3 may be involved in intra- or intermolecular interactions with the N-terminal domain during PrP^{Sc} formation and may influence the ultimate conformational change of the N terminus, perhaps through an altered β -sheet structure. In keeping with this, our IR spectra detected a difference in β -sheet structures between 22L-PrP^{Sc} and Chandler-PrP^{Sc} (Fig. 7). If these distinct N-terminal domains had differing interactions with helices 2 and 3, particularly around residues 185 and 218, then our mutations may have created structural changes that were compatible with only one of the strains. For example, the introduction of Q185R into helix 2 of mouse PrP^c may have interfered with the conformational change of its N-terminal domain into 22L-PrP^{Sc} via steric hindrance and/or electrostatic incompatibility while still allowing its conversion into Chandler-PrP^{Sc}. These strain-specific interactions between the N-terminal domain and helices 2 and 3 are likely quite localized, as mutations at other sites did not reveal any strain differences.

In addition to the location of the mutant residues, the nature of their amino acid change may have contributed to our ob-

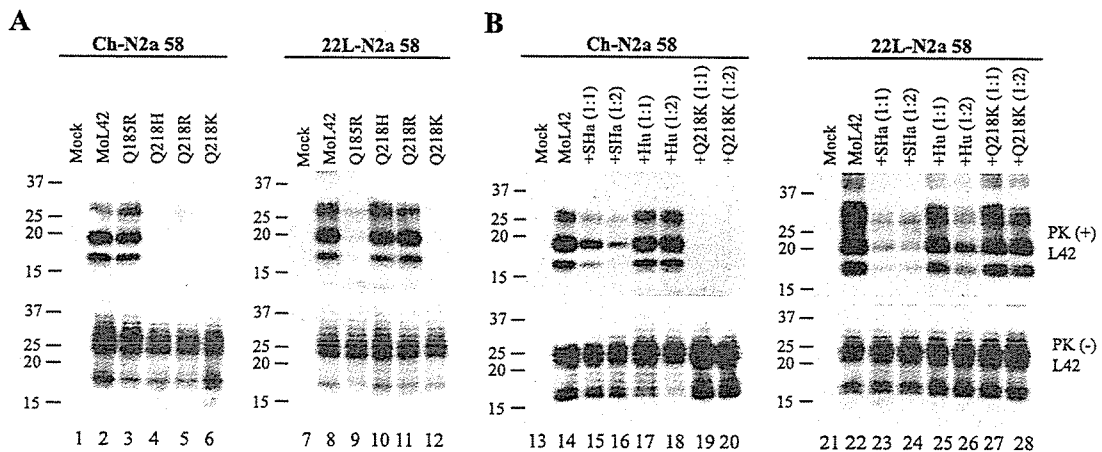


FIG. 5. Strain-specific effects of L42-positive mutated PrPs on PrP^{Sc} formation. (A) Conversion to L42-positive PrP^{Sc} (upper panels) and expression of MoL42, Q185R, Q218H, Q218R, and Q218K (lower panels) were measured by Western blot using L42 antibody. The L42 epitope was present in all these constructs. (B) Inhibitory effects of SHa, Hu, and Q218K were determined by cotransfection with MoL42 at a 1:1 or 1:2 DNA ratio. The blots were probed with the L42 antibody. Molecular mass markers are indicated in kilodaltons on the left side of each panel.

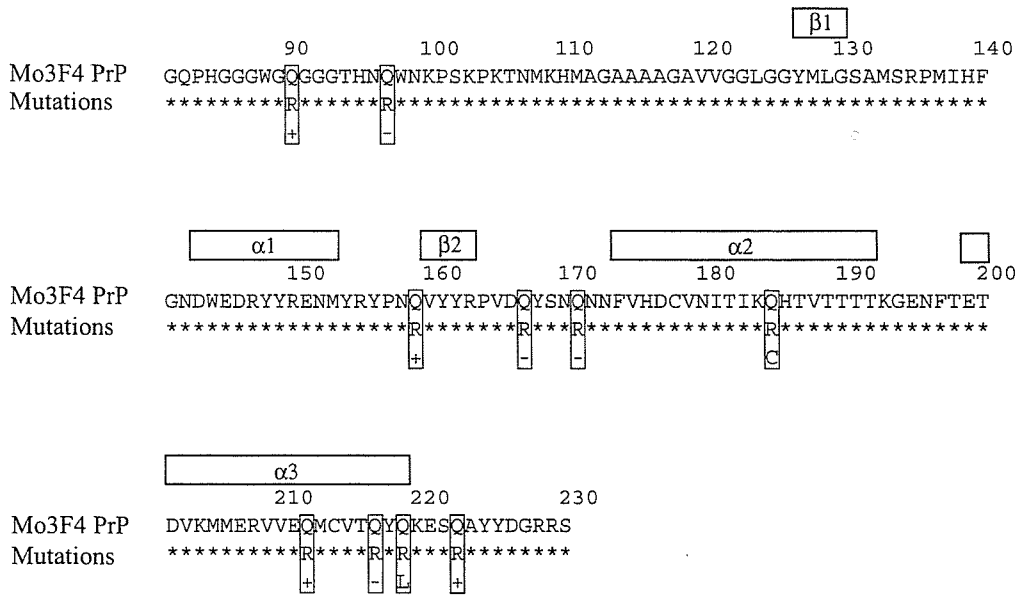


FIG. 6. Amino acid sequence of Mo3F4 and the position of mutations. The amino acid residue number is based on Mo3F4 PrP. The secondary structures in mouse PrP^C are indicated in white boxes at the top. Boxed residues indicate the representative mutations tested; + indicates that conversion occurred in the two cells; - indicates that conversion did not occur in the two cells; "C" indicates Chandler-specific conversion; "L" indicates 22L-specific conversion.

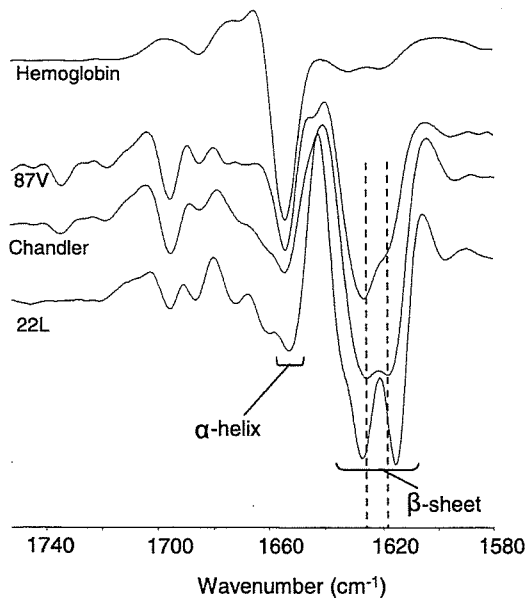


FIG. 7. Comparison of 22L, Chandler, and 87V PrP^{Sc} by infrared spectroscopy. Second-derivative Fourier transform IR spectra are shown for PK-treated PrP^{Sc} samples isolated from the brains of mice affected by either 22L, Chandler, or 87V scrapie. Spectral differences, especially in the β -sheet region of the spectrum, provide evidence that PrP^{Sc} proteins associated with these murine-adapted scrapie strains have distinct conformations. For comparison, a highly α -helical protein, hemoglobin, gives strong absorbance (represented by a negative deflection) at ~ 1657 cm^{-1} , with only minor absorbance in the β -sheet region. Similar results were obtained from at least two independent preparations of each strain of PrP^{Sc}.

servations. Similar mutations have been studied to a great extent in yeast, where the translation termination factor Sup35 can aggregate and self-propagate in a prion-like manner. The introduction of point mutations into Sup35 often prevents its aggregation and can block the phenotype of cells that contain aggregated Sup35 (the yeast prion state or [PSI]) in a dominant inhibitory fashion. Interestingly, random mutagenesis of Sup35 has revealed that most of these mutants have a glutamine or serine replaced with an arginine (18). Likewise, our PrP mutants, which contained an arginine instead of a glutamine, frequently did not convert and also inhibited the conversion of wild-type PrP. The large, charged arginine side chain most likely has a disruptive effect on the protein-protein interactions that are necessary for aggregation and/or conversion.

Another interesting relationship between our study and those of Sup35 is that in both settings, select mutants have shown strain-specific conversion or aggregation behaviors. When Sup35 aggregates, various levels of translation through premature stop codons can occur, which produces different [PSI] phenotypes (53, 58). [PSI] strains are heritable and have distinct biological properties that can be propagated in the same yeast genetic background (20). A few Sup35 mutants that displayed different levels of dominant inhibition of [PSI], depending on the variant to which they were exposed, have been discovered (19, 30), just as our codon 185 and 218 mutants showed different conversion rates depending on the PrP^{Sc} strain to which they were exposed. The analogous results suggest that various prion types may share similar strain determinants.

A second possibility that could account for the strain-specific properties of our PrP mutations is that the alterations affected interactions between PrP and a strain-specific agent or a host factor. The heterodimer model of the protein-only hypothesis

suggests that an as-yet-unidentified host factor, protein X, is responsible for the behavior of a number of dominant inhibitory forms of PrP^c (26, 51). Interestingly, codon 218 is one of the proposed binding sites for protein X; therefore, a mutation at this site should result in similar conversion rates in cells from the same line, which would have the same protein X. However, in our study, there was a dramatic difference in Q218R and Q218H mutant PrP^{Sc} formation in the same cell line infected with either the Chandler or the 22L strain. Moreover, we and others (55) have shown that PrP mutations with inhibitory effects on conversion are not restricted to the proposed protein X binding sites. There are several previous studies that demonstrated the importance of sulfated glycosaminoglycans (5, 12, 46, 48, 59) and the laminin receptor in PrP^{Sc} formation (33), and more recently, in vitro PrP^{Sc} formation experiments using brain homogenates revealed that host-encoded RNA molecules facilitated PrP^{Sc} formation (17). However, to fully explain how the same mutant PrP^c can convert differently when exposed to two PrP^{Sc} strains, any invoked factor must be associated with the strain itself. For example, the virus or virino hypothesis (15, 27, 34) proposes that agent-encoded nucleic acids are the true determinants of strain diversity. Unfortunately, evidence for such nucleic acids is lacking.

It should be noted that the strain-specific effects were not related to cloning artifacts or the influence of introduced epitopes. Our results were reproduced in other clones and mass cultures prior to cloning (data not shown). In addition, changing the epitope tag from 3F4 to L42 in the mutated PrPs did not affect the strain-specific effects on PrP^{Sc} formation (Fig. 5). This indicated that the properties observed were due only to the codon substitutions.

The best explanation for our data lies with the seeding model hypothesis, which proposes that mutated PrP^c, which is unable to convert, forms a heteropolymer with wild-type PrP^c and PrP^{Sc}, which prevents the conversion of both wild-type and mutated PrP^c. Cell-free conversion studies with purified mouse and hamster PrP isoforms have revealed that heterologous PrP^c, which itself cannot convert, can directly interfere with the conversion of homologous PrP^c into PrP^{Sc}. Furthermore, mouse PrP^c can form heteropolymers with hamster PrP^c and PrP^{Sc} and vice versa (24).

In conclusion, we have shown that mutations at codons 185 and 218 in mouse PrP^c reveal strain-specific effects on PrP^{Sc} formation in cell culture. The conversion differences and IR data suggest that distinct conformations underlie the characteristics of these strains, although the presence of an unidentified strain-specific cofactor cannot be excluded. Further study of these mutants may lead to a better understanding of the structure of PrP^{Sc} and the process by which it is formed. This, in turn, will help advance the knowledge of the molecular basis of TSE strains.

ACKNOWLEDGMENTS

We thank Nobuhiko Okimura for technical assistance, Tsuyoshi Mori for support of indirect immunofluorescence of PrP, and Gregory Raymond for providing brain-derived PrP^{Sc}.

This work was supported by the 21st Century COE Program of Nagasaki University and grants from the Ministry of Education, Culture, Sports, Science, and Technology, Japan, and the Ministry of Health, Labor, and Welfare, Japan. V.L.S. acknowledges support from

the Alberta Heritage Foundation for Medical Research through a clinical fellowship award.

REFERENCES

- Alonso, D. O., S. J. DeArmond, F. E. Cohen, and V. Daggett. 2001. Mapping the early steps in the pH-induced conformational conversion of the prion protein. *Proc. Natl. Acad. Sci. USA* 98:2985–2989.
- Arima, K., N. Nishida, S. Sakaguchi, K. Shigematsu, R. Atarashi, N. Yamaguchi, D. Yoshikawa, J. Yoon, K. Watanabe, N. Kobayashi, S. Mouillet-Richard, S. Lehmann, and S. Katamine. 2005. Biological and biochemical characteristics of prion strains conserved in persistently infected cell cultures. *J. Virol.* 79:7104–7112.
- Atarashi, R., N. Nishida, K. Shigematsu, S. Goto, T. Kondo, S. Sakaguchi, and S. Katamine. 2003. Deletion of N-terminal residues 23–88 from prion protein (PrP) abrogates the potential to rescue PrP-deficient mice from PrP-like protein/Doppel-induced neurodegeneration. *J. Biol. Chem.* 278:28944–28949.
- Belt, P. B., I. H. Muileman, B. E. Schreuder, R. Bos-de Ruijter, A. L. Gielkens, and M. A. Smits. 1995. Identification of five allelic variants of the sheep PrP gene and their association with natural scrapie. *J. Gen. Virol.* 76:509–517.
- Ben-Zaken, O., S. Tzaban, Y. Tal, L. Horonchik, J. D. Esko, I. Vlodavsky, and A. Taraboulos. 2003. Cellular heparan sulfate participates in the metabolism of prions. *J. Biol. Chem.* 278:40041–40049.
- Bessen, R. A., D. A. Kocisko, G. J. Raymond, S. Nandan, P. T. Lansbury, and B. Caughey. 1995. Non-genetic propagation of strain-specific properties of scrapie prion protein. *Nature* 375:698–700.
- Bessen, R. A., and R. F. Marsh. 1992. Biochemical and physical properties of the prion protein from two strains of the transmissible mink encephalopathy agent. *J. Virol.* 66:2096–2101.
- Birkett, C. R., R. M. Hennion, D. A. Bembridge, M. C. Clarke, A. Chree, M. E. Bruce, and C. J. Bostock. 2001. Scrapie strains maintain biological phenotypes on propagation in a cell line in culture. *EMBO J.* 20:3351–3358.
- Bruce, M. E. 1993. Scrapie strain variation and mutation. *Br. Med. Bull.* 49:822–838.
- Bruce, M. E. 2003. TSE strain variation. *Br. Med. Bull.* 66:99–108.
- Bruce, M. E., I. McConnell, H. Fraser, and A. G. Dickinson. 1991. The disease characteristics of different strains of scrapie in Sinc congenic mouse lines: implications for the nature of the agent and host control of pathogenesis. *J. Gen. Virol.* 72:595–603.
- Caughey, B., and G. J. Raymond. 1993. Sulfated polyanion inhibition of scrapie-associated PrP accumulation in cultured cells. *J. Virol.* 67:643–650.
- Caughey, B., G. J. Raymond, and R. A. Bessen. 1998. Strain-dependent differences in beta-sheet conformations of abnormal prion protein. *J. Biol. Chem.* 273:32230–32235.
- Caughey, B. W., A. Dong, K. S. Bhat, D. Ernst, S. F. Hayes, and W. S. Caughey. 1991. Secondary structure analysis of the scrapie-associated protein PrP 27–30 in water by infrared spectroscopy. *Biochemistry* 30:7672–7680.
- Chesebro, B. 2003. Introduction to the transmissible spongiform encephalopathies or prion diseases. *Br. Med. Bull.* 66:1–20.
- Collinge, J., K. C. Sidle, J. Meads, J. Ironside, and A. F. Hill. 1996. Molecular analysis of prion strain variation and the aetiology of 'new variant' CJD. *Nature* 383:685–690.
- Deleault, N. R., R. W. Lucassen, and S. Supattapone. 2003. RNA molecules stimulate prion protein conversion. *Nature* 425:717–720.
- DePace, A. H., A. Santoso, P. Hillner, and J. S. Weissman. 1998. A critical role for amino-terminal glutamine/asparagine repeats in the formation and propagation of a yeast prion. *Cell* 93:1241–1252.
- Derkatch, I. L., M. E. Bradley, P. Zhou, and S. W. Liebman. 1999. The PNM2 mutation in the prion protein domain of SUP35 has distinct effects on different variants of the [PSI⁺] prion in yeast. *Curr. Genet.* 35:59–67.
- Derkatch, I. L., Y. O. Chernoff, V. V. Kushnirov, S. G. Inge-Vechtomov, and S. W. Liebman. 1996. Genesis and variability of [PSI] prion factors in *Saccharomyces cerevisiae*. *Genetics* 144:1375–1386.
- Goldfarb, L. G., R. B. Petersen, M. Tabaton, P. Brown, A. C. LeBlanc, P. Montagna, P. Cortelli, J. Julien, C. Vital, W. W. Pendelbury, M. Haltia, P. R. Wills, J. J. Hauw, P. E. McKeever, L. Monari, B. Schrank, G. D. Swergold, L. Autilio-Gambetti, D. C. Gajdusek, E. Lugaresi, and P. Gambetti. 1992. Fatal familial insomnia and familial Creutzfeldt-Jakob disease: disease phenotype determined by a DNA polymorphism. *Science* 258:806–808.
- Herrmann, L. M., and B. Caughey. 1998. The importance of the disulfide bond in prion protein conversion. *Neuroreport* 9:2457–2461.
- Hill, A. F., M. Desbruslais, S. Joiner, K. C. Sidle, I. Gowland, J. Collinge, L. J. Doey, and P. Lantos. 1997. The same prion strain causes vCJD and BSE. *Nature* 389:448–450, 526.
- Horiuchi, M., S. A. Priola, J. Chabry, and B. Caughey. 2000. Interactions between heterologous forms of prion protein: binding, inhibition of conversion, and species barriers. *Proc. Natl. Acad. Sci. USA* 97:5836–5841.
- Jones, E. M., and W. K. Surewicz. 2005. Fibril conformation as the basis of species- and strain-dependent seeding specificity of mammalian prion amyloids. *Cell* 121:63–72.

26. Kaneko, K., L. Zulianello, M. Scott, C. M. Cooper, A. C. Wallace, T. L. James, F. E. Cohen, and S. B. Prusiner. 1997. Evidence for protein X binding to a discontinuous epitope on the cellular prion protein during scrapie prion propagation. *Proc. Natl. Acad. Sci. USA* 94:10069-10074.
27. Kimberlin, R. H. 1982. Scrapie agent: prions or virions? *Nature* 297:107-108.
28. Kimberlin, R. H., S. Cole, and C. A. Walker. 1987. Temporary and permanent modifications to a single strain of mouse scrapie on transmission to rats and hamsters. *J. Gen. Virol.* 68:1875-1881.
29. Kimberlin, R. H., C. A. Walker, and H. Fraser. 1989. The genomic identity of different strains of mouse scrapie is expressed in hamsters and preserved on reisolation in mice. *J. Gen. Virol.* 70:2017-2025.
30. King, C. Y. 2001. Supporting the structural basis of prion strains: induction and identification of [PSI] variants. *J. Mol. Biol.* 307:1247-1260.
31. King, C. Y., and R. Diaz-Avalos. 2004. Protein-only transmission of three yeast prion strains. *Nature* 428:319-323.
32. Korth, C., K. Kaneko, D. Groth, N. Heye, G. Telling, J. Mastrianni, P. Parchi, P. Gambetti, R. Will, J. Ironside, C. Heinrich, P. Tremblay, S. J. DeArmond, and S. B. Prusiner. 2003. Abbreviated incubation times for human prions in mice expressing a chimeric mouse-human prion protein transgene. *Proc. Natl. Acad. Sci. USA* 100:4784-4789.
33. Leucht, C., S. Simoneau, C. Rey, K. Vana, R. Rieger, C. I. Lasmezas, and S. Weiss. 2003. The 37 kDa/67 kDa laminin receptor is required for PrP(Sc) propagation in scrapie-infected neuronal cells. *EMBO Rep.* 4:290-295.
34. Manuelidis, L. 2003. Transmissible encephalopathies: speculations and realities. *Viral Immunol.* 16:123-139.
35. Meyer, R. K., M. P. McKinley, K. A. Bowman, M. B. Braunfeld, R. A. Barry, and S. B. Prusiner. 1986. Separation and properties of cellular and scrapie prion proteins. *Proc. Natl. Acad. Sci. USA* 83:2310-2314.
36. Muramoto, T., M. Scott, F. E. Cohen, and S. B. Prusiner. 1996. Recombinant scrapie-like prion protein of 106 amino acids is soluble. *Proc. Natl. Acad. Sci. USA* 93:15457-15462.
37. Nishida, N., D. A. Harris, D. Vilette, H. Laude, Y. Frobert, J. Grassi, D. Casanova, O. Milhavet, and S. Lehmann. 2000. Successful transmission of three mouse-adapted scrapie strains to murine neuroblastoma cell lines overexpressing wild-type mouse prion protein. *J. Virol.* 74:320-325.
38. Pan, K. M., M. Baldwin, J. Nguyen, M. Gasset, A. Serban, D. Groth, I. Mehlhorn, Z. Huang, R. J. Fletterick, F. E. Cohen, and S. B. Prusiner. 1993. Conversion of alpha-helices into beta-sheets features in the formation of the scrapie prion proteins. *Proc. Natl. Acad. Sci. USA* 90:10962-10966.
39. Peretz, D., M. R. Scott, D. Groth, R. A. Williamson, D. R. Burton, F. E. Cohen, and S. B. Prusiner. 2001. Strain-specified relative conformational stability of the scrapie prion protein. *Protein Sci.* 10:854-863.
40. Peretz, D., R. A. Williamson, Y. Matsunaga, H. Serban, C. Pinilla, R. B. Bastidas, R. Rozenshteyn, T. L. James, R. A. Houghten, F. E. Cohen, S. B. Prusiner, and D. R. Burton. 1997. A conformational transition at the N terminus of the prion protein features in formation of the scrapie isoform. *J. Mol. Biol.* 273:614-622.
41. Prusiner, S. B., M. R. Scott, S. J. DeArmond, and F. E. Cohen. 1998. Prion protein biology. *Cell* 93:337-348.
42. Riek, R., S. Hornemann, G. Wider, M. Billeter, R. Glockshuber, and K. Wuthrich. 1996. NMR structure of the mouse prion protein domain PrP(121-321). *Nature* 382:180-182.
43. Riek, R., G. Wider, M. Billeter, S. Hornemann, R. Glockshuber, and K. Wuthrich. 1998. Prion protein NMR structure and familial human spongiform encephalopathies. *Proc. Natl. Acad. Sci. USA* 95:11667-11672.
44. Safar, J., H. Wille, V. Itri, D. Groth, H. Serban, M. Torchia, F. E. Cohen, and S. B. Prusiner. 1998. Eight prion strains have PrP(Sc) molecules with different conformations. *Nat. Med.* 4:1157-1165.
45. Scott, M., D. Foster, C. Mirenda, D. Serban, F. Coufal, M. Walchli, M. Torchia, D. Groth, G. Carlson, S. J. DeArmond, D. Westaway, and S. B. Prusiner. 1989. Transgenic mice expressing hamster prion protein produce species-specific scrapie infectivity and amyloid plaques. *Cell* 59:847-857.
46. Shaked, G. M., Z. Meiner, I. Avraham, A. Taraboulos, and R. Gabizon. 2001. Reconstitution of prion infectivity from solubilized protease-resistant PrP and nonprotein components of prion rods. *J. Biol. Chem.* 276:14324-14328.
47. Shibuya, S., J. Higuchi, R. W. Shin, J. Tateishi, and T. Kitamoto. 1998. Codon 219 Lys allele of PRNP is not found in sporadic Creutzfeldt-Jakob disease. *Ann. Neurol.* 43:826-828.
48. Snow, A. D., R. Kisilevsky, J. Willmer, S. B. Prusiner, and S. J. DeArmond. 1989. Sulfated glycosaminoglycans in amyloid plaques of prion diseases. *Acta Neuropathol. (Berlin)* 77:337-342.
49. Tanaka, M., P. Chien, N. Haber, R. Cooke, and J. S. Weissman. 2004. Conformational variations in an infectious protein determine prion strain differences. *Nature* 428:323-328.
50. Telling, G. C., P. Parchi, S. J. DeArmond, P. Cortelli, P. Montagna, R. Gabizon, J. Mastrianni, E. Lugaresi, P. Gambetti, and S. B. Prusiner. 1996. Evidence for the conformation of the pathologic isoform of the prion protein enciphering and propagating prion diversity. *Science* 274:2079-2082.
51. Telling, G. C., M. Scott, J. Mastrianni, R. Gabizon, M. Torchia, F. E. Cohen, S. J. DeArmond, and S. B. Prusiner. 1995. Prion propagation in mice expressing human and chimeric PrP transgenes implicates the interaction of cellular PrP with another protein. *Cell* 83:79-90.
52. Thomzig, A., S. Spassov, M. Friedrich, D. Naumann, and M. Beekes. 2004. Discriminating scrapie and bovine spongiform encephalopathy isolates by infrared spectroscopy of pathological prion protein. *J. Biol. Chem.* 279:33847-33854.
53. Uptain, S. M., and S. Lindquist. 2002. Prions as protein-based genetic elements. *Annu. Rev. Microbiol.* 56:703-741.
54. Vorberg, I., A. Buschmann, S. Harmeyer, A. Saalmuller, E. Pfaff, and M. H. Groschup. 1999. A novel epitope for the specific detection of exogenous prion proteins in transgenic mice and transfected murine cell lines. *Virology* 255:26-31.
55. Vorberg, I., M. H. Groschup, E. Pfaff, and S. A. Priola. 2003. Multiple amino acid residues within the rabbit prion protein inhibit formation of its abnormal isoform. *J. Virol.* 77:2003-2009.
56. Weissmann, C. 2004. The state of the prion. *Nat. Rev. Microbiol.* 2:861-871.
57. Westaway, D., V. Zuliani, C. M. Cooper, M. Da Costa, S. Neuman, A. L. Jenny, L. Detwiler, and S. B. Prusiner. 1994. Homozygosity for prion protein alleles encoding glutamine-171 renders sheep susceptible to natural scrapie. *Genes Dev.* 8:959-969.
58. Wickner, R. B., H. K. Edskes, B. T. Roberts, U. Baxa, M. M. Pierce, E. D. Ross, and A. Brachmann. 2004. Prions: proteins as genes and infectious entities. *Genes Dev.* 18:470-485.
59. Wong, C., L. W. Xiong, M. Horiuchi, L. Raymond, K. Wehrly, B. Chesebro, and B. Caughey. 2001. Sulfated glycans and elevated temperature stimulate PrP(Sc)-dependent cell-free formation of protease-resistant prion protein. *EMBO J.* 20:377-386.

プリオン病の治療

— その現状と展望 —

逆瀬川裕二 堂浦克美

SAKASEGAWA Yuji, DOH-URA Katsumi/東北大学大学院医学系研究科プリオン蛋白分子解析分野

プリオン病は、いまだ有効な治療法がない、発症すると確実に死に至る進行性の神経変性疾患である。現在、プリオン本体およびその感染のメカニズムについて急速に理解が進んでいるが、治療薬・治療法についてはいまだ有効なものが見出されていない。英国を中心に欧州で新たに出現した変異型クロイツフェルト・ヤコブ病は、現在小康状態にあるものの、血液製剤を介して二次感染の可能性も考えられている。プリオン病の発症前での診断・検査法、そして予防薬・治療薬の早急な開発が求められている。

はじめに

プリオン病あるいは伝達性海綿状脳症(transmissible spongiform encephalopathy; TSE)は進行性の神経変性疾患であり、有効な治療法が確立されていない現在、治療不可能の致死性の難病となっている。孤発性クロイツフェルト・ヤコブ病(Creutzfeldt-Jakob disease; CJD)を代表とするヒトプリオン病は、年間100万人に1人の割合で発症し、その多くのものは数週間から数ヶ月で急激に症状が進行し、死に至る。発症すると、脳内に海綿状の神経変性ととともにプリオンと呼ばれる感染性を持つ蛋白質(PrP^{Sc})の蓄積を生じる。ヒトプリオンが実験動物へと感染し得ることは以前よりよく知られていたが、1980年代に英国を中心に蔓延していた牛海綿状脳症(bovine spongiform encephalopathy; BSE)が、1996年、ヒトへも経口感染し、

新たなヒトプリオン病、変異型CJDを引き起こすことが報道されると、欧州全体を巻き込んだ大きなパニックを引き起こした。わが国でもBSE感染牛が2001年に発見され、2005年には英国旅行者の邦人1人が変異型CJDであることが確認された。また、米国や日本ではプリオンに感染した硬膜などの生体材料の移植によって医原性CJDが発生し、特にわが国では対策の遅れもあり、100人を超える症例が報告され、薬害ヤコブ病として大きな社会問題となっている。

現在、プリオン病に対する理解が進み、また感染防止対策がうまく機能していることもあり、BSEや変異型CJDの発生は小康状態あるいは減少へと転じている。しかし、発症していないにもかかわらず感染性を有する、いわゆるキャリアの存在と、血液製剤を介した変異型CJDの二次感染の例が報告され、今後、変異型CJDの発生が拡大していく可能性も出てきた。

Key words

プリオン病
クロイツフェルト・ヤコブ病
治療
予防

近年、プリオン病の基礎研究や治療薬のスクリーニング・検出技術に大きな進展があり、いくつかの薬剤についてはすでに臨床試験にて検討されているが、有効なプリオン病予防薬および治療薬の開発までには至っていない。

プリオン病とは

プリオン病は通常のウイルスや細菌の感染とは異なり、プリオンと呼ばれる蛋白質によって感染が引き起こされる¹⁾。プリオンはプロテアーゼや高熱に耐性を持つ、不溶性の異常感染型プリオン蛋白(PrP^{Sc})である。生体には同じアミノ酸配列からなる正常プリオン蛋白(PrP^C)と呼ばれる膜蛋白が存在する。これらの蛋白質の高次構造(コンフォメーション)は大きく異なり、PrP^{Sc}はβシートに富み、アミロイドと呼ばれる不溶性の多量体を形成するが、PrP^Cはαヘリックスに富む可溶性の単量体として存在する。ヒトにおいては、特定のアミノ酸置換や挿入を持つPrP^C変異体が知られており、PrP^{Sc}の感染の有無にかかわらずプリオン病を自然発症する(遺伝性プリオン病)、外科手術などの医療行為よりPrP^{Sc}に汚染された生体材料より感染する場合もある。しかし、ヒトプリオン病の8割は孤発性であり、その原因は不明である。動物実験では、感染体と同じアミノ酸配列を持つPrP^Cを導入することや、PrP^Cを過剰発現させることによって、感染しやすくなることが知られている。プリオン病は、人

獣共通感染症として知られるが、PrP^{Sc}と同じアミノ酸配列を持つPrP^Cを発現させることによって、異なる種間の感染をより簡単に成立させることも可能になっている。PrP^C、PrP^{Sc}以外の宿主因子の存在も指摘されているが、現在のところ不明である。PrP^Cの存在はプリオン感染の成立だけでなく、神経変性にも必須であり、感染に付随する神経変性の原因は脳、神経に蓄積するPrP^{Sc}というよりも、PrP^CからPrP^{Sc}へと構造変換する過程で生じるという説が有力である。

治療薬スクリーニング法の開発

プリオン病の治療薬の開発には、プリオン持続感染培養細胞を用いてPrP^{Sc}の産生量を測定するアッセイ法と、プリオンを接種したハムスターやマウスの潜伏期の長さを指標にしたアッセイ法が主に用いられている。最近になって、酵母プリオンを用いた方法や、*in vitro*で起こるPrP^CからPrP^{Sc}様のプロテアーゼ耐性産物を測定する方法も開発され、治療薬スクリーニングに利用されている。

培養細胞を用いる方法²⁾は、多数の検体を安価に迅速に処理することが可能である。最近では、サブクロニングによって高いプリオン感染能を持つ細胞を使用し、さらにメンブレンフィルターに転写することによって、多検体を迅速に定量的に測定できるように改良されている³⁾。しかし、培養細胞で認められた治療効果が、動物実験で

は必ずしも再現できない場合が多く、多検体からの一次スクリーニングとして使用されることが多い。

動物を用いたバイオアッセイは、感染価をエンドポイント希釈することによって発症を指標に測定する方法(IC₅₀)や、感染価と潜伏期の長さが反比例関係にあることを利用して感染価を測定する方法を用いて、感染価を推定することができる。これまで開発されたプリオン検出系の中で最も感度が良いことが知られているが、確定するのに時間と費用がかかることが欠点である。ハムスターを用いたバイオアッセイ⁴⁾は、プリオン仮説の提唱者である Prusiner によって採用され、プリオンの精製の際に使用された。このハムスターを用いたバイオアッセイは、最短60日で感染を検出できるバイオアッセイであったが、PrP^Cを過剰発現するトランスジェニックマウスの開発によって、ほぼ同等に潜伏期を短縮することに成功している。加えて、PrP^{Sc}と同じアミノ酸配列を有するPrP^Cを発現するように作製されたトランスジェニックマウスによって、種の異なるプリオン感染も再現できるようになった。また、腹腔内にプリオンを接種後、感染初期にPrP^{Sc}の蓄積が認められる脾臓中のPrP^{Sc}の産生を測定することによって、感染を30日で検出することも可能になっている⁵⁾。

その他に、[PSI+]や[URE3]という酵母プリオンを用いたスクリーニング系⁶⁾や、PrP^CとPrP^{Sc}の相互作用を蛍光相関分光法を用いて測定するハイスループットスクリーニング法⁷⁾や、

表面プラズモン共鳴法による PrP^Cとの相互作用を利用したスクリーニング法⁹⁾が新たに開発されている。

高感度プリオン検出法の開発

PrP^{Sc}の検出法には、プロテアーゼ処理によって混在する PrP^Cを除去し、プロテアーゼ耐性の PrP^{Sc}をメンブレンあるいはプレート上で免疫化学的に測定するウェスタンブロット法や ELISA 法が従来使用されてきた。その後、PrP^{Sc}に特異性を持つポリマーでコーティングしたプレートを用いる ELISA 法や、コンフォメーションを認識する抗体を用いた ELISA 法 (CDI 法)⁹⁾など、プロテアーゼ処理を省略した検出法も開発されている。また、PrP^{Sc}との相互作用によってコンフォメーション変化を起こし、蛍光を発するよう工夫されたペプチドを用いた高感度検出法や、DNA の増幅に使われている PCR 法によく似た原理によって *in vitro* で PrP^{Sc}を増幅すると

いう検出法 (PMCA 法)¹⁰⁾など、新しい原理による検出法も開発されている。PMCA 法は、PrP^{Sc}からなる凝集体がある条件下で PrP^Cを重合して、より大きな PrP^{Sc}凝集体を形成することを利用して、一定時間ごとに超音波処理と重合反応を繰り返すことにより PrP^{Sc}を増幅するという方法で、これまで最も感度の良かったバイオアッセイをしのぐ感度を有しており、ごく低濃度の PrP^{Sc}の検出などにおいて、現在最も高感度の測定法となっている。現在のところ、増幅できるプリオンは限定されるなど、まだ克服すべき点があるが、反応の自動化も完了しており、血液や尿など低濃度のプリオンを含む試料の高感度検出とプリオン病の早期発見への応用に期待されている。

プリオン病の治療薬候補

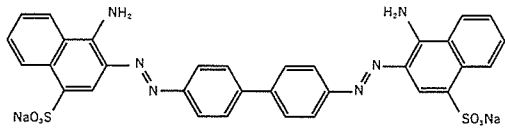
プリオン病の治療薬候補として、多くの薬剤、化合物が報告されている。最近になって、さまざまなアッセイ系

によってこれまでスクリーニングされたプリオン病予防薬・治療薬について体系的に検討された結果が、Brain 誌に報告されている¹¹⁾ので参照されたい。

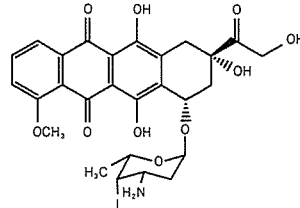
- ① アミロイド結合性を持つ Congo red¹¹⁾,
- ② 抗アミロイド活性を持つ抗癌剤ヨードドキシソルピシン (4'-deoxy-4'-iododoxorubicin ; IDOX)¹²⁾とその構造類似体のテトラサイクリン (tetracycline)¹³⁾,
- ③ 抗ウイルス薬からスクリーニングによって見出されたアンフォテリシン B (amphotericin B ; AmB)¹⁴⁾などのポリエン系抗生物質,
- ④ アミロイド結合性を持つペントサンポリサルフェート (pentosan polysulfate ; PPS)¹⁵⁾などのポリアニオン誘導体,
- ⑤ アミロイドなどの β シート構造を破壊するペプチド¹⁶⁾,
- ⑥ 蛋白質と結合し、立体構造に変化を与えるポルフィリン (porphyrin) などのテトラピロール類¹⁷⁾,
- ⑦ 特定の構造を持つトランスフェクシ

表 1 プリオン病治療薬候補

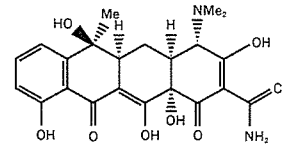
プリオン病治療薬候補化合物	化合物名	発見の経緯、化合物の特徴
アミロイド結合性化合物	Congo red	アミロイド結合性
四環系化合物	IDOX, テトラサイクリン	抗癌剤, 抗アミロイド活性
ポリエン系抗生物質	アンフォテリシン B	抗ウイルス薬よりスクリーニング
ポリアニオン系化合物	ペントサンポリサルフェート	同上
β シート破壊ペプチド	iPrP13	アミロイド構造の破壊
テトラピロール系化合物	FeTSP	蛋白質構造変化促進, Congo red 様構造
ポリアミン化合物	PAMAM	トランスフェクション試薬, 抗プリオン作用
三環系化合物	キナクリン, クロルプロマジン	抗マラリア薬, 抗精神病薬, BBB 透過
抗体, 免疫賦活剤	抗 PrP 抗体 6H4, D18	PrP ^C への結合
その他	メマンチン, フルビルチン	NMDA 受容体アゴニスト, 抗神経細胞死



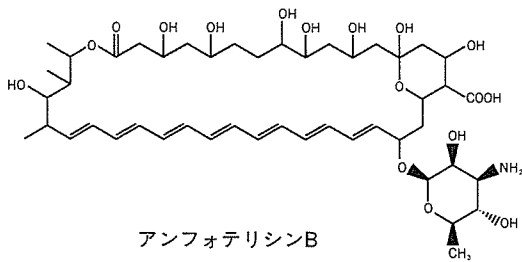
Congo red



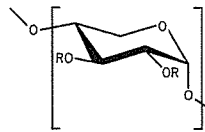
ヨードキソルピシン



テトラサイクリン



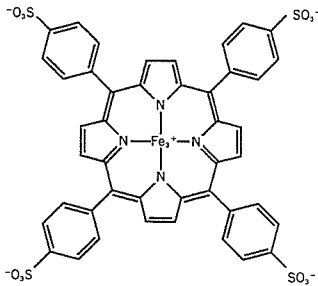
アンフォテリシンB



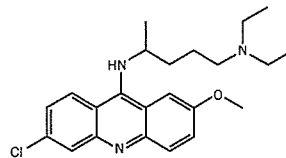
ペントサンポリサルフェート
(R=SO₃Na, n=12)

PrP^{115A} AA AG AV V¹²²
iPrP13 DAPAAPAGPAVPV

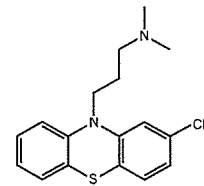
βシート破壊ペプチド



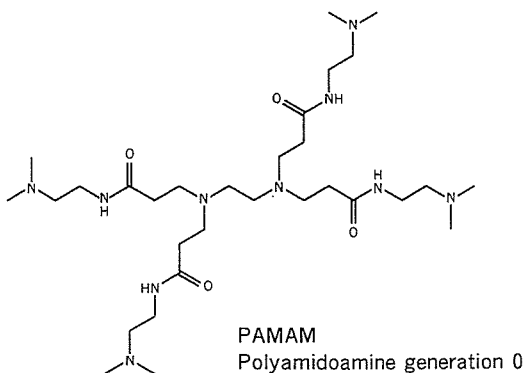
FeTSP
Iron (III) meso-tetra (4-sulphonatophenyl) Porphine



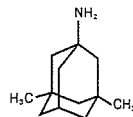
キナクリン



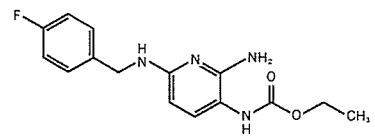
クロルプロマジン



PAMAM
Polyamidoamine generation 0



メマンチン



フルピルチン

図1 さまざまなプリオン病治療薬

オン試薬が抗プリオン活性を示すこと
から見出された分岐性ポリアミン、
⑧抗プリオン蛋白抗体¹⁰⁾、
⑨血液脳関門(BBB)を透過する既存
の治療薬からスクリーニングにより
見つかった抗マラリア薬キナクリン
(quinacrine)¹⁸⁾や抗精神薬クロルプ
ロマジン(chlorpromazine)¹⁹⁾など、
⑩神経細胞死を抑制する薬剤から
NMDA 受容体拮抗薬メマンチン
(memantine)²⁰⁾や中枢性鎮痛薬フ
ルピルチン(flupirtine)²⁰⁾、
などがある(表1, 図1)。これらのな
かで、実際に患者に應用されている薬
剤および化合物には、AmB, PPS,
キナクリン、フルピルチンなどがある。
本稿では、キナクリン、PPS および
フルピルチンについて解説する。

キナクリンは、長年にわたって抗マ
ラリア薬として広く使用されてきた薬
剤であり、安全性も高いことから、米
国、フランス、英国などにて臨床研究
が進められている。わが国においても
孤発性CJD 22例、医原性CJD 5例、
遺伝性プリオン病4例の計31例の症
例に対し、300 mg/day を経口、ある
いは経管投与にて12週間の連続投与
というプロトコルで臨床研究が行われ
た。その結果、12例で覚醒度や自
発語、注視など、臨床症状に一過的な
改善が認められたが(効果が認められ
た例: 孤発性9例、医原性2例、遺伝
性1例)、その後、効果は消失した。
16例に肝機能障害や溶血性貧血など
の重大な副作用が認められ、より毒性
の低い塩酸キニーネに変更されたが、
持続的な薬効を保つことと副作用を抑

えることが困難であった²¹⁾。

PPSについては、英国を中心に13
例の治療が行われてきた。わが国では
福岡大学にて臨床試験が行われてい
る²²⁾。PPSはBBBを透過しないため、
微量注入器具を用いて脳室内へ連続投
与することが検討され、動物実験では
脳内接種後10日からの投与で173%、
30日からの投与で93%の潜伏期の延
長が認められた¹⁵⁾。本薬剤は、2003
年、英国において1例の変異型CJD
患者にて臨床研究が開始されたが、脳
の萎縮の進行は止まらなかったものの
副作用は認められず、臨床症状は落ち
着いており、現在まだ経過を観察中だ
る。わが国でも、さまざまなプリオン
病患者で臨床研究が開始されており、
その効果と副作用について解析が進め
られている²³⁾。PPSを用いた脳室内
持続投与療法は、英国や日本以外の国
でも開始され、全世界で20例近い患
者に実施されており、現在最も期待さ
れている治療法のひとつといえる。今
後、最適の治療プロトコルの完成と、
臨床症状の改善が判断できる症例での
検討が求められる。

フルピルチンは、非オピオイド系の
中枢性鎮痛薬として臨床で用いられて
きたが、細胞培養実験などから神経細
胞死を抑制する効果が再発見されて以
来、神経変性疾患への治療に應用され
ようになってきた。CJD患者につ
いては、28名の患者において二重盲
検試験として臨床試験が行われた²⁴⁾。
その結果、フルピルチンはCJDの認
知機能の低下を有意に抑制したものの、
CJDの進行を抑制することはできな

かった。

おわりに

プリオン病は通常の細菌やウイルス
などを介した感染症と異なり、感染し
てからの潜伏期が長く、発症直前まで
感染の有無を知ることができない。加
えて、急速に進む神経変性を治療して
いくことは非常に難解な問題となっ
ている。末梢から中枢神経への感染を予
防することは、現在開発されているい
くつかの薬剤でも可能と思われるが、
それには発症前に治療を開始するこ
とが必須であり、現在のところ、医原性
プリオン病や遺伝性プリオン病など、
将来発症する可能性のある人には応用
することができるものの、実際的では
ない。MRI 拡散強調画像や脳脊髄液
中の14-3-3蛋白質などが神経変性初
期の診断の助けになることが報告され
ているが、より早い時期での診断のた
めのマーカーの検索や検出法の開発が
求められている。血液や尿中のPrP^{Sc}
の高感度検出は、感染初期あるいは発
症初期の検出法となるかもしれない。
従来、PrP^{Sc}が神経変性の原因と考え
られていたが、いくつかの実験から、
PrP^CあるいはPrP^CからPrP^{Sc}に変化
する中間体が神経変性を引き起こすと
の仮説が提唱されている。必ずしも
PrP^{Sc}の増殖を防げなくとも、神経変
性のメカニズムを明らかにし、神経変
性の進行を抑制する薬剤の探索や治療
法を開発することは、プリオン病の治
療法のひとつのゴールでもある。ここ
らの展開にも期待したい。